PEOPLE'S DEMOCRATIC REPUBLIC OF ALGERIA

MINISTRY OF HIGHER EDUCATION AND SCIENTIFIC RESEARCH

UNIVERSITY KASDI MERBAH - OUARGLA-

FACULTY OF HYDROCARBONS, RENEWABLE ENERGIES, AND EARTH AND UNIVERSE SCIENCES

Dissertation

Academic Master

Domain: Earth Sciences

Field: Geology

Specialty: Geology of Sedimentary Basins

Presented by

Hadjer MESSAOUDI

Environmental Geochemistry of P-bearings from The Tebessa deposits

Defended publicly on: 04. 06. 2026

IN FRONT OF

Mr. Mohamed Salah BELKSIER	Prof.	UKM-Ouargla	President
Mr. Rabah KECHICHED	Prof.	UKM-Ouargla	Supervisor
Ms. Safia SAOULI	Dr.	UKM-Ouargla	Co-Supervisor
Mr. Abdellatif REMITA	MAA	UKM-Ouargla	Examiner

Academic Year: 2025/2026

Dedication

To those who have been my support every step of the way, to my beloved family the source of love, encouragement, and reassurance.

To my dear parents, **Maaradj Messaoudi.** and **Oum Elkheir Ghdayer Ahmed**, who instilled in me the values of perseverance, patience, and determination, and who have always been my greatest source of encouragement and prayers.

To my brothers and sisters **Mohamed, Abd Raouf, Abdelkader, Saadia, Chaima, Salsabil, Israa, Ahmed Abdelhay, and Yacine Abdelbari** who shared with me moments of hardship and hope, stood by my side throughout the different stages of my life, and continually supported me with their love and encouragement.

I dedicate this humble work to all of you as a token of my love, gratitude, and appreciation for your unwavering moral support. I sincerely hope that this achievement is worthy of you and of the special place you hold in my heart.

I would also like to express my sincere gratitude and deep appreciation to my wonderful supervisor, **Dr. Safia Saouli**, the pride and flower of Ouargla University, for her continuous support, valuable guidance, and unwavering dedication. Her constant encouragement, patience, commitment to scientific rigor, and continuous follow-up played a crucial role in overcoming difficulties and completing this work to the best of my ability.

I pray to Almighty Allah to bless her with good health, success in her teaching and research career, and abundant knowledge. May Allah reward her with the best of rewards for all that she has done.

HDJER

Acknowledgments

I would like to begin by expressing my profound gratitude to my dissertation supervisor, **Prof. Rabah KECHICHED**, whose guidance, expertise, and unwavering support were instrumental throughout this research journey. His insightful advice helped refine my scientific skills and sharpen the focus of my research. I am deeply grateful for the confidence, motivation, and perseverance he inspired in me, enabling me to successfully complete this dissertation. His extensive knowledge and experience in phosphate geology greatly enriched this work, and collaborating with him has been both scientifically rewarding and personally inspiring. I sincerely thank him for his patience, encouragement, professionalism, and exceptional dedication to the successful completion of this dissertation.

My sincere appreciation is also extended to **Ms. Safia SAOULI**, co-supervisor of this work, for her valuable guidance, constructive suggestions, and continuous support throughout the preparation and development of this dissertation.

I am honored to express my heartfelt thanks to the distinguished members of the jury for accepting to evaluate this dissertation. In particular, I am grateful to **Prof. BELKSIER Mohamed Salah**, President of the Jury from Kasdi Merbah University of Ouargla, and **Dr. REMITA Abdel Latif**, Examiner from Kasdi Merbah University of Ouargla. Their valuable comments, insightful observations, and constructive criticisms have significantly contributed to improving the quality of this work.

I would also like to acknowledge **Mr. Omar GADJA**, Engineer at the Sahara Geology Laboratory of the Scientific Research Center of Ouargla, and **Prof. Messaoud HACINI**, Director of the Sahara Geology Laboratory, for their invaluable assistance and technical support during the X-ray diffraction (XRD) analyses.

Finally, I extend my deepest gratitude to my family and friends for their constant encouragement, patience, and unwavering belief in me. Their frequent inquiries about the progress of my dissertation, although sometimes challenging during moments of uncertainty, served as a source of motivation and a constant reminder to remain committed to my goals and persevere until the completion of this work.

Table of Contents

LIST OF Figures

LIST OF TABLES

Abstract

Sedimentary phosphorite deposits from the Kef Essenoun sector of the Djebel Onk Basin constitute an important phosphate resource formed during the Paleocene–Eocene interval in northeastern Algeria. This study presents an integrated petrographic, granulometric, mineralogical, geochemical, and environmental assessment of these phosphorites in order to characterize their depositional evolution, mineralogical composition, trace-element distribution, and associated ecological implications. Fifteen (15) phosphorite samples representing basal, main, and upper stratigraphic sub-layers were investigated using petrographic observations, grain-size analysis, X-ray diffraction (XRD), and ICP-MS geochemistry approaches.

Petrographic investigations reveal that the phosphorites are mainly composed of pellets and coprolites, accompanied by glauconite, phosphoclasts, and biogenic fragments embedded within a micritic to dolomitic matrix. Evidence of reworking, silicification, and dolomitization reflects intense depositional and early diagenetic processes. Grain-size analyses indicate polymodal to monomodal distributions with clear vertical variations between stratigraphic sub-layers. The basal layer is characterized by poorly sorted coarse sediments deposited under relatively high-energy conditions, whereas the upper layer displays finer and better-sorted grains indicative of low-energy and more stable marine environments. XRD analyses demonstrate the predominance of carbonate-fluorapatite (CFA), associated with carbonate-hydroxylapatite, calcite, dolomite, quartz, gypsum, clinoptilolite, and glauconite. Fine fractions are enriched in clay minerals and glauconite, suggesting reducing depositional conditions and significant diagenetic alteration.

Geochemistry confirms high CaO (>40 wt.%) and P_2O_5 contents (up to 34.25 wt.%), together with substantial enrichment in trace metal elements (TMEs), particularly Sr, Y, Cr, Zn, Cd, and U. Environmental assessment indices reveal extremely high enrichment factors for Cd and U, with Cd reaching EF values up to 49,600. Geo-accumulation index (I-geo) and Potential Ecological Risk Index (PERI) results indicate that the phosphorites represent a considerable to very high ecological risk, particularly near the Paleocene-Eocene boundary, where intensified redox fluctuations, enhanced marine productivity, and climatic perturbations promoted trace-element accumulation. These findings demonstrate that the Kef Essenoun phosphorites preserve

strong sedimentological and geochemical signatures of depositional and diagenetic evolution while also constituting a potential environmental concern due to the enrichment of toxic trace elements. The study emphasizes the importance of selective exploitation and sustainable waste-management strategies to minimize ecological and human-health risks associated with phosphorite mining and processing.

Keywords: phosphorite; carbonate-fluorapatite; petrography; grain-size analysis; XRD; trace metal elements; ecological risk; Paleocene-Eocene; Djebel Onk Basin.

Résumé

Les dépôts phosphatés sédimentaires du secteur de Kef Essenoun, appartenant au bassin de Djebel Onk, constituent une importante ressource phosphatée formée durant l'intervalle Paléocène-Éocène dans le nord-est de l'Algérie. Cette étude présente une approche intégrée pétrographique, granulométrique, minéralogique, géochimique et environnementale de ces phosphorites afin de caractériser leur évolution sédimentaire, leur composition minéralogique, la distribution des éléments traces ainsi que leurs implications écologiques. Quinze (15) échantillons de phosphorites représentant les sous-couches stratigraphiques basale, principale et supérieure ont été étudiés à l'aide d'observations pétrographiques, d'analyses granulométriques, de diffraction des rayons X (DRX) et d'analyses géochimiques par ICP-MS.

Les investigations pétrographiques montrent que les phosphorites sont principalement constituées de pellets et de coprolithes, accompagnés de glauconite, de phosphoclastes et de fragments biogéniques inclus dans une matrice micritique à dolomitique. Les phénomènes de remaniement, de silicification et de dolomitisation témoignent de processus sédimentaires et diagénétiques précoces intenses. Les analyses granulométriques indiquent des distributions allant de polymodales à monomodales avec des variations verticales nettes entre les sous-couches stratigraphiques. La couche basale est caractérisée par des sédiments grossiers mal triés déposés dans des conditions relativement énergétiques, tandis que la couche supérieure présente des grains plus fins et mieux triés, indiquant un environnement marin plus calme et stable. Les analyses DRX montrent la dominance de la carbonate-fluorapatite (CFA), associée à la carbonate-hydroxylapatite, à la calcite, à la dolomite, au quartz, au gypse, à la clinoptilolite et à la glauconite. Les fractions fines sont enrichies en minéraux argileux et en glauconite, suggérant des conditions de dépôt réductrices et une altération diagénétique importante.

Les analyses géochimiques confirment des teneurs élevées en CaO (>40 % poids) et en P_2O_5 (jusqu'à 34,25 % poids), ainsi qu'un enrichissement marqué en éléments traces métalliques (ETM), notamment Sr, Y, Cr, Zn, Cd et U. Les indices d'évaluation environnementale révèlent des facteurs d'enrichissement extrêmement élevés pour le Cd et l'U, avec des valeurs EF atteignant 49 600 pour le Cd. Les résultats de l'indice de géoaccumulation (I-geo) et de l'indice de risque écologique potentiel (PERI) indiquent que ces phosphorites représentent un risque écologique considérable à très élevé, particulièrement à proximité de la limite Paléocène–

Éocène, où les fluctuations redox, l'augmentation de la productivité marine et les perturbations climatiques ont favorisé l'accumulation des éléments traces. Ces résultats montrent que les phosphorites de Kef Essenoun conservent des signatures sédimentologiques et géochimiques marquées liées à l'évolution dépôt-diagenèse, tout en constituant une source potentielle de contamination environnementale en raison de l'enrichissement en éléments traces toxiques. Cette étude souligne l'importance d'une exploitation sélective et de stratégies durables de gestion des déchets afin de réduire les risques écologiques et sanitaires liés à l'exploitation et au traitement des phosphorites.

Mots-clés : phosphorites ; carbonate-fluorapatite ; pétrographie ; analyse granulométrique ; DRX ; éléments traces métalliques ; risque écologique ; Paléocène-Éocène ; bassin de Djebel Onk.

الملخص

تُعد رواسب الفوسفوريت الرسوبية في قطاع كاف السنون ضمن حوض جبل العنق من أهم الموارد الفوسفاتية المتشكلة خلال الفترة الممتدة بين الباليوسين والإيوسين في شمال شرق الجزائر. تقدم هذه الدراسة تقييماً متكاملًا بتروغرافياً، وحبيبياً، ومعدنياً، وجيوكيميائياً، وبيئياً لهذه الفوسفوريتات بهدف توصيف تطورها الترسيبي، وتركيبها المعدني، وتوزيع العناصر النزرة، وانعكاساتها البيئية. شملت الدراسة خمسة عشر (15) عينة من الفوسفوريت تمثل الطبقات القاعدية والرئيسية والعلوية، حيث تم تحليلها باستخدام الملاحظات البتروغرافية، والتحليل الحبيبي، وحيود الأشعة السينية(XRD) ، والتحاليل الجيوكيميائية بتقنية.ICP-MS

أظهرت الدراسات البتروغرافية أن الفوسفوريتات تتكون أساساً من الحبيبات الفوسفاتية (Pellets) والكوبروليتات، إضافة إلى الغلوكونيت، والفتات الفوسفاتي، والبقايا الحيوية ضمن مصفوفة ميكراتية إلى دولوميتية. كما تعكس مظاهر إعادة الترسيب والسيليسة والدلمتة تأثير العمليات الرسوبية والتحولات الدياجينية المبكرة. وأظهرت التحاليل الحبيبية توزيعات تتراوح بين متعددة النمط وأحادية النمط مع تباينات عمودية واضحة بين الطبقات. تتميز الطبقة القاعدية برسوبيات خشنة وضعيفة الفرز ترسبت في بيئة ذات طاقة مرتفعة نسبياً، في حين تتميز الطبقة العلوية بحبيبات أدق وأكثر تجانساً وفرزاً، مما يدل على بيئة بحرية هادئة وأكثر استقراراً. وأكدت تحاليل XRD سيادة معدن الكربونات-فلورأباتيت(CFA) ، مصحوباً بالكربونات- هيدروكسي أباتيت، والكالسيت، والدولوميت، والكوارتز، والجبس، والكلينوبتيلوليت، والغلوكونيت. كما أظهرت الكسور الدقيقة غنىً بالمعادن الطينية والغلوكونيت، مما يشير إلى ظروف ترسيب مختزلة وتحولات دياجينية ملحوظة.

أكدت التحاليل الجيوكيميائية ارتفاع محتوى % 40>) CaO وزناً و) P_2O_5حتى 34.25 % وزناً)، إضافة إلى إثراء واضح بالعناصر النزرة المعدنية، خاصة Sr و Yو Crو Znو Cdو .Uكما كشفت مؤشرات التقييم البيئي عن معاملات إثراء مرتفعة جداً لكل من Cd وU، حيث بلغت قيم معامل الإثراء (EF) للكادميوم حوالي 49,600. وأظهرت نتائج مؤشر التراكم الجيولوجي (I-geo) ومؤشر المخاطر البيئية المحتملة (PERI) أن هذه الفوسفوريتات تمثل خطراً بيئياً مرتفعاً إلى مرتفع جداً، خصوصاً بالقرب من الحد الفاصل بين الباليوسين والإيوسين، حيث ساهمت التغيرات في ظروف الأكسدة والاختزال، وارتفاع الإنتاجية البحرية، والاضطرابات المناخية في تراكم العناصر النزرة. وتبرز هذه النتائج أن فوسفوريتات كاف السنون تحتفظ ببصمات رسوبية وجيوكيميائية واضحة مرتبطة بالتطور الترسيبي والدياجيني، كما قد تشكل مصدراً محتملًا للتلوث البيئي نتيجة الإثراء بالعناصر النزرة السامة. وتؤكد الدراسة أهمية الاستغلال الانتقائي واعتماد استراتيجيات مستدامة لإدارة النفايات من أجل الحد من المخاطر البيئية والصحية المرتبطة باستغلال ومعالجة الفوسفوريت.

الكلمات المفتاحية :الفوسفوريت؛ الكربونات-فلورأباتيت؛ البتروغرافيا؛ التحليل الحبيبي؛ حيود الأشعة السينية؛ العناصر النزرة المعدنية؛ المخاطر البيئية؛ الباليوسين-الإيوسين؛ حوض جبل العنق.

INTRODUCTION GENERAL

Phosphorus is naturally widespread in the environment and represents one of the essential nutrients for the sustainability of plant and animal life, together with potassium (K)and nitrogen (N). It also plays a fundamental role in plant metabolism, thereby contributing to plan growth and development. In terms of applications, phosphorites are widely exploited in numerous sectors, being primarily consumed in the manufacture of phosphate fertilizers. They also constitute an important raw material in several industrial fields, including the chemical, metallurgical, and pharmaceutical industries (Van Kauwenbergh, 2010), furthermore phosphorites hold considerable scientific importance in sedimentary geology, as they provide valuable records of the geological and geochemical timescales (Follmi, 1996).

Form a geochemical perspective, sedimentary phosphorites are characterized by the presence of wide range of trace elements, including Uranium (U), Cadmium (Cd), lead (Pb) Zinc (Zn), as well as rare earth elements (REEs) (Altschule, 1980). Although these elements generally occur at low concentration in the Earth is crust, they may become significantly enriched within phosphorite deposits as a result of sedimentary and diagenetic processes (Jarvis et al., 1994). This enrichment raises important scientific and environmental concerns related to understanding the geochemical pathways controlling their distribution. Moreover, the extraction, processing, and extensive exploitation of phosphorite ores have generated major environmental concerns due to the dispersion of trace metal elements (TMEs) into soils and groundwater during mining activities, industrial processing, and the application of phosphorite-based fertilizers, thereby posing potential environmental and human health risks (Boumaza et al., 2024).

This study investigates potentially toxic elements in phosphorites, using the Kef Essenoun deposit as an example, which is currently exploited for phosphate raw materials. The study includes chapters dedicated to generalities, regional and local geology, petrography, petrographic, grain-size, and mineralogical analyses, as well as geochemical and environmental implications. The results will help characterize potentially toxic elements and may support more rational environmental management and health protection.

CHAPTER 1: GENERALITIES

GHAPTER 1: GENERALITES

Introduction

Natural phosphates are considered an important mineral resource for global agriculture and industrial development (Filippelli, 2008). Phosphorus, the principal constituent of phosphorite minerals, is a chemical element belonging to group 5 of the periodic table with the atomic number 15 (Farr, 1950) (Fig.1).

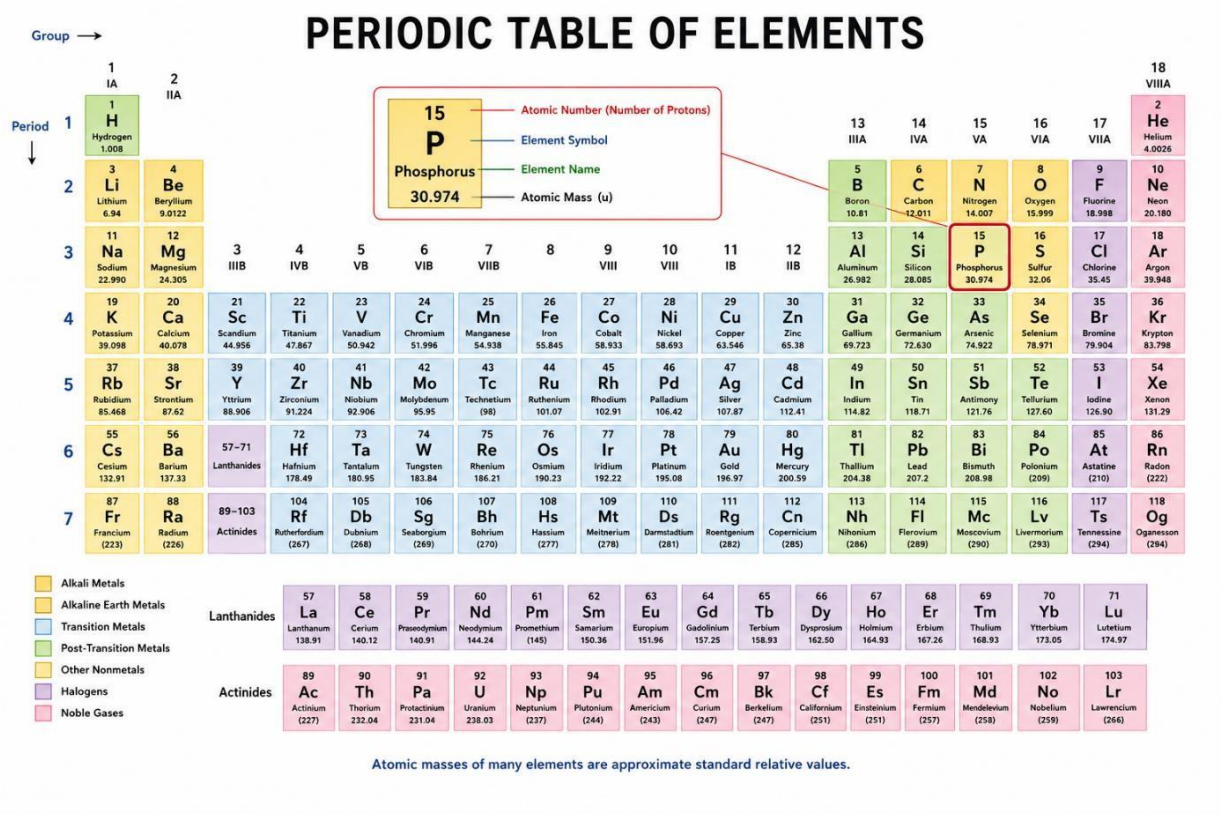

Figure 1: Phosphorus in the periodic table.

1. Generalities on phosphorus and phosphorites

1.1. Historical background of phosphorus

The term phosphorus originates from the Greek word meaning light-bearer, in reference to planet Venus, also known as the morning star.

Phosphorus was discovered by the German chemist Henning Brand in 1669, when he conducted a series of experiments including: He evaporated large quantities of urine, and after several attempts, he succeeded in isolating a glowing waxy substance from the urine, which was later

found to be elemental phosphorus (Ashley et al, 2011). In 1777, phosphorus was listed among the chemical elements. Since then, studies on this element have seen significant development, including a study Ive and Jenkins 1973 on phosphorus in aquatic environments and the mitigation of algal bloom phenomena, furthermore, Steck conducted a specialized study in 1980 on the biochemistry of phosphorus, in which he compounds and the analytical methods related to then.

1.2. Phosphorus properties

Phosphorus (P) is classified among the pnictogen elements, Group 15 of the periodic table, and has an atomic number of 15. It has an electron configuration of $1s^2\ 2s^2\ 2p^6\ 3s^2\ 3p^3$, and its outer energy level contains three unpaired electrons in the 3p orbitals it to form chemical bonds (Figure 2).

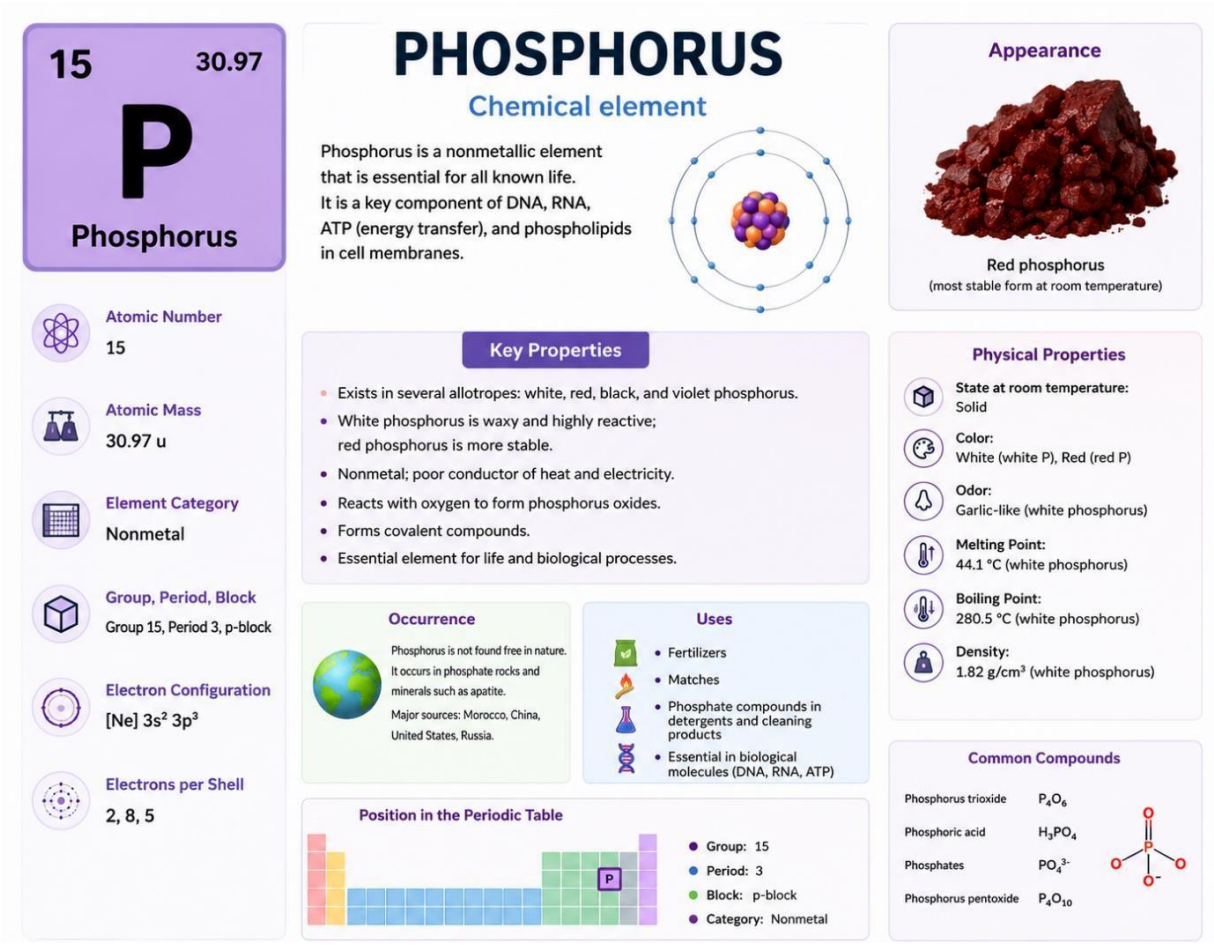

Figure.2: Electronic properties of the Phosphorus (P) element.

1.3. The Phosphorus cycle

Phosphorus is an essential that limits primary biological productivity over geological limescales (Tyrrell, 1999). unlike most other biogeochemical cycles, the phosphorus cycle has no gaseous phase and is not connected to the atmosphere (Corbridge, 2016), (Figure. 3). Instead, its cycling

occurs between the lithosphere, hydrosphere, and biosphere. In Earth early history, phosphorus was primarily found within igneous rocks. The phosphorus cycle begins when rocks are exposed to weathering, which releases inorganic phosphate ions into the environment. these ions are then transported to soils and various aquatic system. Phosphorus reaches the oceans through riverine and atmospheric inputs. In its inorganic form, orthophosphate (-PO_4^{3}), it is taken up by marine photoautotrophs and converted into organic phosphorus compounds. Upon the death of these organisms, they decompose, and phosphorus is recycled back into seawater, while another portion contributes to the formation of the mineral apatite within phosphate deposits (Follmi, 1996).

For terrestrial plants, phosphorous is absorbed by plants and other organisms. After these organisms die, they decompose through microbial degradation, releasing phosphorus back into the soil. A portion of this phosphorus can be transported to marine environments, where it subsequently participation in the formation of phosphate deposits (Follmi, 1996; Ruttenberg, 2003).

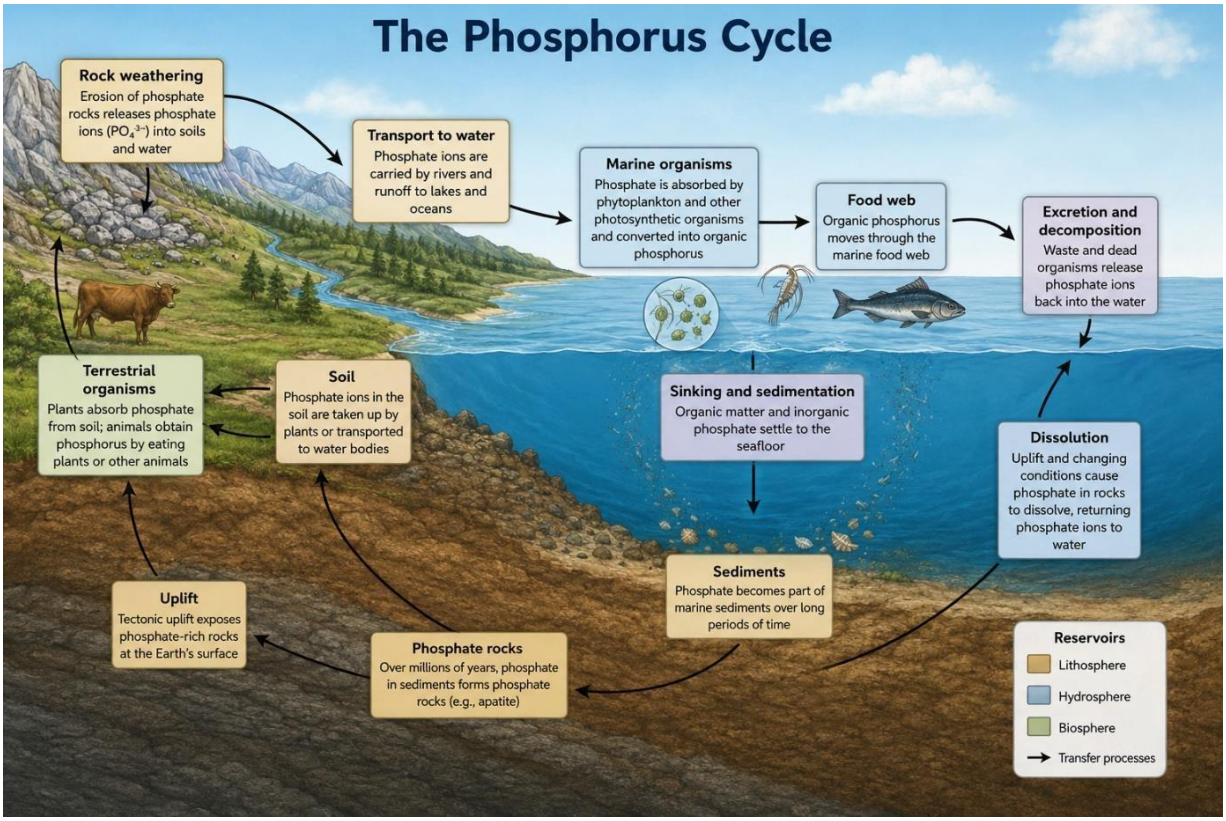

Figure. 3: The phosphorus (KatherineC. Ruttenberg, 2001,2019).

1.4. Phosphorus deposits

Phosphate deposits are classified into three main types: igneous deposits, sedimentary deposits, and guano deposits. igneous deposits are generally associated with carbonatite rocks, which are characterized by their high content of carbonate minerals, constituting up to 50% of the rock volume. Sedimentary phosphates are considered biochemical deposits rich in essential elements such as phosphorus, iron, and silicon. They typically form as a result of biochemically mediated precipitation processes.

Most sedimentary phosphates originate in upwelling zones, where deep, phosphorus rich waters rise toward the shelf. In this environment, phytoplankton absorb the phytoplankton absorb the Phosphorus brought to surface waters. Subsequently, through the accumulation and decomposition of organic matter, this element is transformed into apatite minerals within phosphate deposits.

The original source of dissolved phosphorus traces back to the chemical weathering of continental rocks, which indicates the interconnection between igneous and sedimentary deposits within the geochemical phosphorus cycle. Sedimentary rocks containing more than 18wt.%phosphorite rocks.

Guano deposits, on the other hand, form as a result of the accumulation of seabird excrement and its reaction with the underlying calcareous rocks, leading to the formation of calcium phosphates(Pohl and Groat and ,2017; Slansky, 1986; Nathan,1984).

1.4.1. Igneous deposits

Igneous phosphorite deposits are widespread in several regions of the world, with geological ages ranging from the Precambrian to the Tertiary. These deposits are typically associated with intrusive alkaline rocks, such as nepheline syenite, carbonatite, and alkaline ultramafic complexes, where they often occur as cylindrical bodies or ring complexes.

Although many of these deposits are characterized by small size and limited economic viability, some are mined commercially and contribute approximately 16% of global phosphorite rock production (Shaban, 2016). These apatite-rich deposits reflect the geographical distribution of alkaline igneous provinces. However, the presence of alkaline rocks does not necessarily imply the availability of economic concentration of apatite. For example, the Khibiny Complex in the kola peninsula, Russia, is known for its significant apatite enrichment, whereas the adjacent Lovero Complex, deposits its geological similarity, lacks deposits of economic value. Thus, the presence of alkaline formations is not a sufficient indicator of exploitable apatite deposits. Nevertheless, the temporal and spatial distribution of igneous phosphorite deposits corresponds

closely with the distribution of alkaline igneous formations, particularly within continental shields, continental platform areas, and rift valley environments (Shaban, 2016).

1.4.2. Sedimentary deposits

Sedimentary phosphorite deposits generally consist of marine accumulation rich phosphorus. Advances in marine geology and oceanography-particularly studies of modern phosphatic depositional environment, along with geochemical analyses of sediments and waters-have enhanced the scientific understanding of the mechanisms controlling the formation and evolution of these deposits (Glenn et al, 1994). Through theses studies, sedimentary phosphates have been identified on several continents, having of formed from the precambrian to the present day. However, most deposits of major economic importance date to the Phanerozoic Eon (Figure 4).

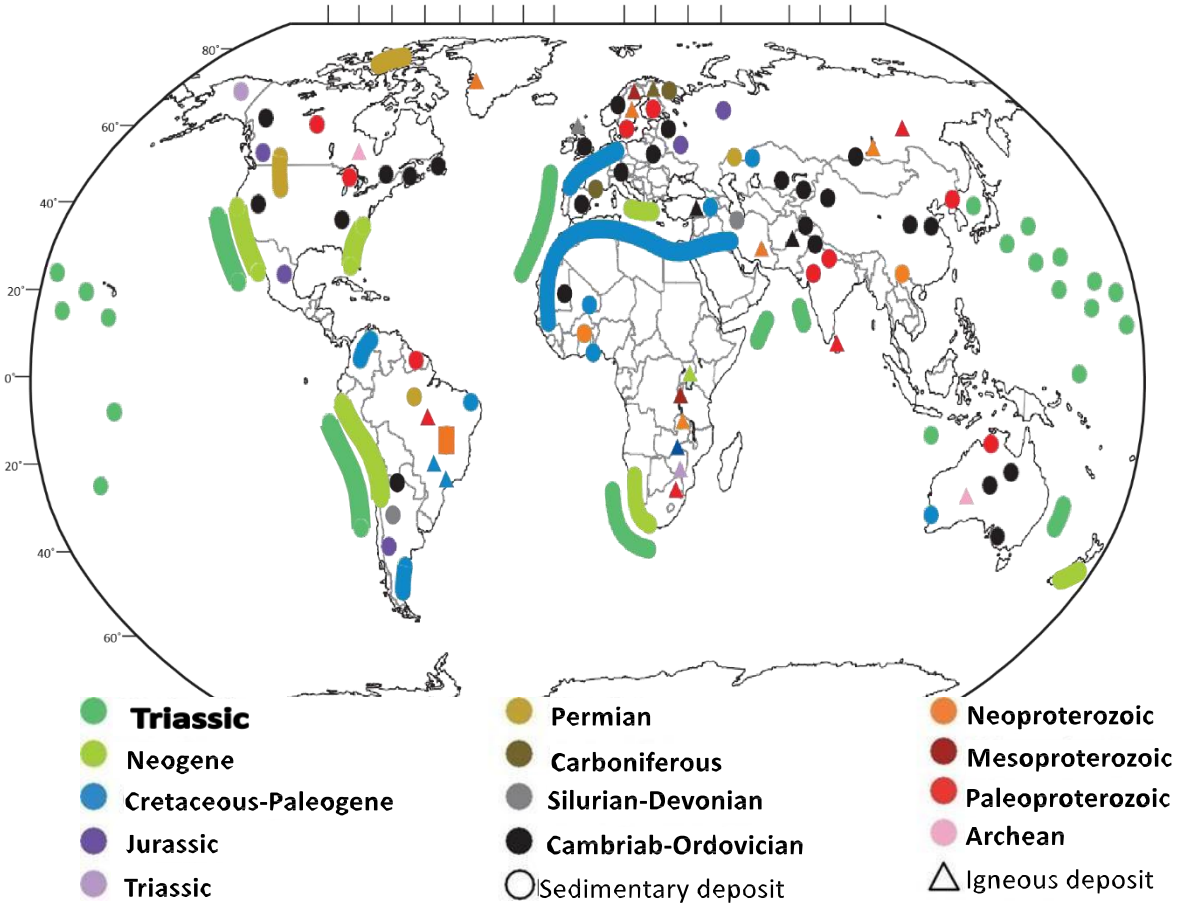

Figure.4: Known igneous and sedimentary phosphorites with respective ages. Copiled from cook and Shergold (1986), NOTHOLT et al. (1989). Burnett and Riggs (1990). Glenn et al. (1994). And Jasinski (2024) (a map from Pufohl and Groat (2017)).

1.4.3. Guano deposits

Guano deposits are among the smallest types of phosphorite resources in terms of volume, yet they retain considerable geological and economic importance. These deposits originate from the decomposition of seabird excrement, which contains about 4% phosphorus. Theses organic materials react with underlying calcareous rock, leading to the formation of calcium phosphate, thereby contributing to the enrichment of phosphate deposits. One of the most significant phosphate deposits of this type in the world is Nauru Island in the Pacificocean, which is of guano origin (Slansky, 1986).

1.5. Geology of sedimentary phosphorites

1.5.1. Introduction to sedimentary phosphorites

Sedimentary phosphorites are considered the most widespread and exploited type of phosphate deposits worldwide (Cook and Shergold, 1984; Notholt et al., 1989). These deposits are mainly composed of calcium phosphate, particularly apatite, which occurs within siliciclastic, carbonate, or clay-rich sediments (Altschuler et al., 1958: Glenn et al., 1994; Follmi, 1996). The distribution of phosphorite is generally associated with shallow marine environment that provided suitable physical and chemical condition for the accumulation and concentration of phosphate minerals. Sedimentary phosphorites commonly form in areas characterized by high biological productivity, such as nutrient-rich upwelling zones. In this environment, the decomposition of organic matter and subsequent diagenetic processes play a major role in the precipitation of phosphate minerals (Cook and McElhinny, 1979; Filippelli, 2011; Jarvis et al., 1994). Although phosphorites have been known since ancient times, their large-scale exploitation began during the nineteenth century with the development of industrial agriculture and the increasing demand for phosphate fertilizers (Follmi. 1996; Glenn et al., 1994). Among the major phosphorite-producing countries worldwide are: Morocco, Tunisia, Chaina, and the United States (Van Kauwenbergh, 2010; Follmi, 1996). Understanding the geological processes responsible for the formation of sedimentary phosphorites is essential for mineral exploration, as well as for studying the concentration of strategic elements such as rare earth elements and uranium, in addition to assessing the environmental impacts associated with the extraction and exploitation of these deposits (Filippelli, 2008; Glenn et al., 1994; Notholt et al 1989).

This literature review focuses on three main themes:

1. The geology of sedimentary phosphorites and their formation mechanisms.
2. Metallic trace elements in terms of their sources, uses, and environment impacts.

3. The geochemical behaviours of metallic trace elements and the environment challenges associated with their occurrence in phosphorite deposits (Filippelli, 2008; Van Kauwenbergh, 2010).

1.5.2. Phosphogenesis and early diagenetic transformations

Phosphogenesis refers to the set of geochemical and biological processes responsible for converting dissolved phosphorus in seawater into solid phosphate minerals, particularly apatite, leading to the formation of sedimentary phosphorite deposits (Altschuler et al., 1958; Sheldon,1964; Cook and McElhinny, 1979; Glenn et al., 1994; Follmi, 1996; Filippelli,2011). These processes occur under interrelated physical, chemical, biological, and diagenetic conditions that affect the marine water column and the sediment-water interface. Phosphorus is transported to marine environments primarily through continental weathering and riverine input, resulting in relatively low concentrations in seawater, estimated at approximately 2-3 µmol/L (Sheldon, 1963; Filippelli, 2011). However, certain environmental condition promotes the local concentration of phosphorus and enhance its mineral precipitation. One of the most important of this condition is coastal upwelling where deep, nutrient-rich waters rise to the surface, leading to increased primary biological productivity and the accumulation of organic matter in marine sediments. Upon decomposition of this organic matter, phosphorus is released within the sediments, creating favorable condition for apatite precipitation and phosphorite formation (Cook and McElhinny, 1979; Follmi, 1996). Anaerobic conditions and reducing environments also contribute by limiting the degradation of organic phosphorus, allowing its accumulation within sediments and subsequent precipitation as phosphate minerals (Altschuler et al., 1958). In addition, alkaline PH values, chemical saturation states, and low sedimentation rates are fundamental factors that increase the stability of phosphorite and enhance its precipitation, especially in condensed marine environments (Follmi, 1996; Filippelli, 2011). Microbial processes play an important role in phosphogenesis, as sulfate-reducing bacteria and phosphogenic bacteria modify redox condition within sediments and may directly participate in the formation of phosphate mineral (Lucas and Prevot, 1981; Glenn et al., 1994). Furthermore, interactions between organic matter and minerals influence phosphorus availability and the mechanisms of phosphate mineral crystallization (Follmi, 1996). Following initial precipitation, phosphorus-rich sediments undergo early diagenesis, which alters their chemical and mineralogical properties. This stage is characterized by the gradual transformation of amorphous or poorly crystallin phases into more stable forms of carbonate fluorapatite (CFA)

(Nancollas et al., 1979; Gunnars et al., 2004; Omelon and Grynpas, 2008). During this transformation, ion exchange occurs between pore waters and phosphatic grains, allowing the incorporation of element such as fluoride, carbonate, and trace elements into the apatite crystal structure, which directly affects the chemical stability and economic value of the deposits (Filippelli,2011).

organic-rich microenvironments, resulting from microbial activity and sulfate reduction, promote local recrystallization of phosphorite (Arning et al 2012). Studies have also shown that microbial mats and sulfide-oxidizing bacteria can catalyze the nucleation of primary apatite minerals, particularly in Miocene phosphorites (Baily et al., 2009; Krajewski,2011).

Thes early diagenetic processes are reflected in the development of distinctive textural features, such as nodules, crusts, and condensed phosphorite-rich beds, which are common characteristics of many global phosphorite deposits across various geological periods (Filippelli, 2011; Arning et al., 2012).

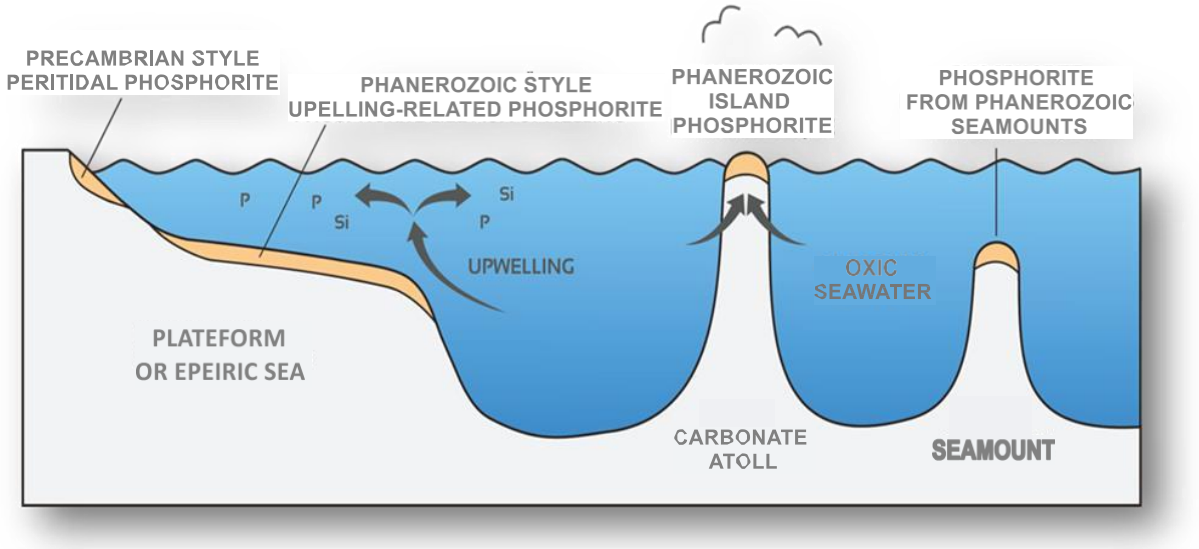

Figure. 5: Deposition environments for sedimentary phosphates Majorass deposits are accumulated on marine platforms and epicontinental seas (Pufahl ang Groat, 2017).

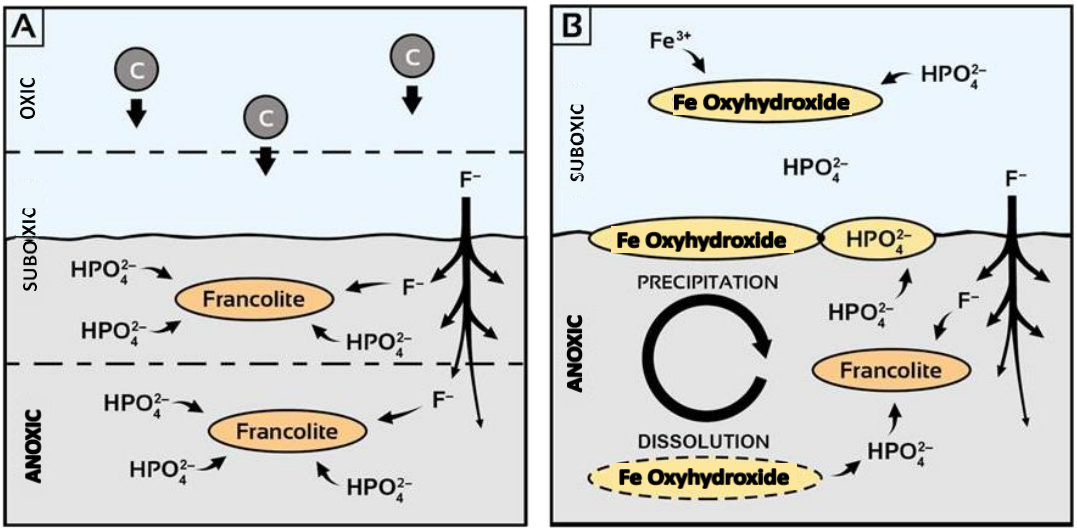

Figure. 6: Phosphatogenesis process.

A): Environment with upwellings where microbial degradation of organic matter.

B): Role of iron oxyhydroxides in pumping phosphorus and maintaining high concentration of this element that will allow francolite precipitation in environments without upwelligs (Pufahl and Groat, 2017).

C): In the sediment, the concentration of dissolved phosphate in the interstital water increases, provoking the precipitation of francoliite. This precipitation is limited at depth by the diffusion of seawater derived F-.

1.5.3. Types of sedimentary phosphorites

Phosphatic lithofacies exhibit considerable variation in their characteristics, reflecting the diversity of sedimentary environments in which they form. Several classifications, schemes have been developed to interpret this variability, including modifications of the Dunham classification, due to the clear similarities between the depositional environments of carbonate rock and phosphorites (Trapp,1998). The genetic classification is among the most widely adopted, as it is based on sediment transport dynamic and the nature of allochemical components. According to this classification, sedimentary phosphorites are divided into two main types: Pristine phosphorite and Reworked phosphorite (Follmi, 1996, 2016; Glenn et al., 1994; Pufahl et al., 2003; Pufahl and Groat, 2017; Trappe, 1998)

2. Toxicity of trace metal elements (TMEs)

2.1. Definition of trace metal elements (TMEs)

Trace Metal Elements (TMEs) are a group of chemical elements that occur naturally in the Erth crust, water, atmosphere, and living organisms, and are characterized by their presence at low concentrations, typically less than 0.1% by weigh (Alloway, 2012). These elements include metals and metalloids, such as (Cu, Zn, Ni, Cd, Pd, As, Ga, V, Sr, Rb, Mo, Cs, U, Cr, Be, As, Nb, Tl, Th, Ba, Sn) (Adriano, 2001). Some trace metal elements play an essential biological role as micronutrients necessary for biological and enzymatic processes, such as iron, copper, and zinc. However, elevated concentration can render them toxic to living organisms (Duffus, 2002). In contrast, other elements have no known biological function, such as cadmium, lead, and mercury, and are considered toxic even at low concentrations (Jarup, 2003). the hazard posed by these elements does not depend solely on their total concentration but is also influenced by their chemical speciation, mobility, and bioavailability-factors that control their degree of toxicity and environmental impact (Alloway, 2012). Therefore, trace metal element receives considerable attention in environmental and geochemical studies due to their importance in assessing pollution and environmental risks.

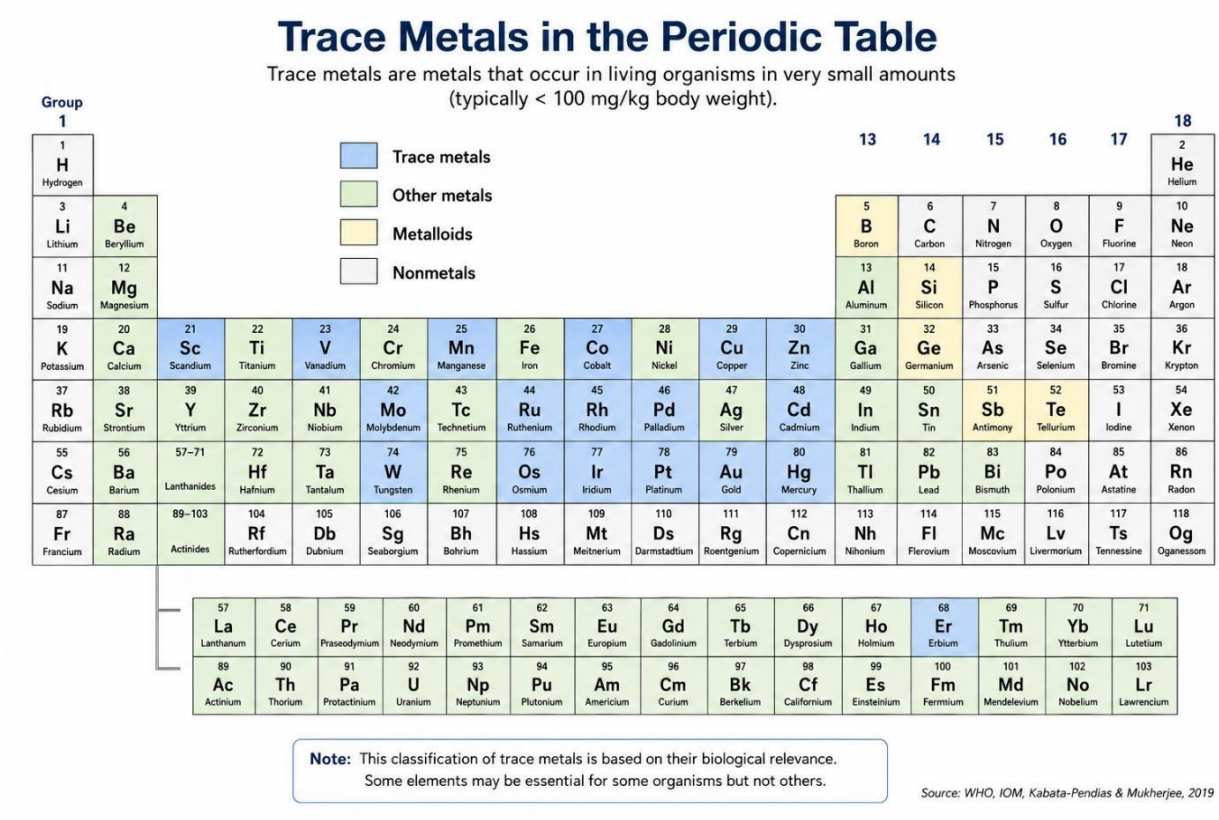

Figure.7: Trace metals in the periodic table

2.1.1. Environmental impacts of trace metal Elements (TMEs)

Trace metal elements are characterized by their high persistence in the environment and potential toxicity, making then a major source of ecosystem degradation and a threat to human health. Their hazard lies in their capacity for bioaccumulation and transfer through food chains, in addition to their role in causing long-term pollution that affects biodiversity and the quality of natural resources.

2.1.2. Mobility and transport of trace metal elements in soil and water

Serval environmental factors control the mobility and transport of trace metal elements within soil and aquatic systems, most notably PH, organic matter, soil texture, and redox conditions (Bradl, 2005; Kabata-Pendias, 2011). Acidic soils increase the solubility of heavy metals and enhance their leachability into ground water (Alloway, 2012; Bradl,2005).

Organic matter can either immobilize these elements or increase their mobility, depending on the nature of chemical interaction (Fermar and Louenco, 2000). Clay minerals and iron and manganese oxides play an important role in adsorbing trace metals and limiting their transport, whereas anaerobic conditions can lead to the release of certain metals and increase their bioavailability (Bradl, 2005; Sposito,2008). Collectively, these processes influence the behavior and distribution of trace metal elements in the environment, which in turn affects soil and water quality and the health of living organisms (Alloway, 2012; Bradl, 2005).

3. Trace metal elements (TMEs) in sedimentary phosphorites

3.1. Natural occurrence of TMEs in phosphorites

Sedimentary phosphates represent one of the most important natural reservoirs of trace metal elements in the geological environment (El-Hasan, 2006; Boumaza et al., 2021). During phosphate formation, these elements accumulate and become incorporated into phosphorite minerals, especially apatite, through several mechanisms such as ionic substitution and surface adsorption (Altschuler, 1980; Glenn et al., 1994; Boumaza et al., 2021).

The geochemical composition of phosphorite deposits is influenced by several key factors:

- The prevailing chemical conditions in the depositional basin, such as PH, oxidation-reduction potential (Eh), and the concentration of dissolved metal ions, control the type and

amounts of trace metal elements accumulated within the deposits (Glenn et al., 1994; Boumaza et al., 2021).

- Detrital inputs and hydrothermal fluids contribute additional trace metal elements, thereby modifying the original geochemical signature of the deposits (Glenn et al., 1994; Pirajno, 2008).
- Diagenetic processes also affect the redistribution of trace metal elements or increase their concentration within the phosphorite matrix through recrystallization and mineral reorganization and mineral reorganization (Koschinsky, 1997; Boumaza et al., 2021).

Studies have shown that sedimentary phosphates are characterized by enrichment in numerous trace metal such as (U, Sr, Cd, Zn, V, Th, Ba, Cu, Ni, Cr, in addition to Rare Earth Elements (REE) (Altschuler, 1998; Glenn et al., 1994; Boumaza et al., 2021).

This enrichment is related to the crystal structure of apatite: $Ca_5 (PO_4)_3(F, Cl, OH)$.

This structure allows for the substitution of numerous metal elements. Therefore, phosphorites are considered an important geochemical record that reflects the depositional and geochemical conditions of the environment. From environmental perspective, the release of these metal elements during the exploitation, processing and production of phosphate fertilizers may lead to the contamination of water and soil (Jiano, 2012; Boumaza et al, 2021)

CHAPTER 2: GEOGRAPHY AND REGEONAL AND LOCAL GEOLOGY

CHPTER 2: GEOGRAPHY AND REGIONAL AND LOCAL GEOLOGY

Introduction

In this chapter, we will highlight the geographical location of the study area within its regional framework of the Eastern Saharan Atlas of Algeria. Understanding the geological framework is crucial for interpreting the processes controlling phosphorite formation and the distribution of associated trace elements. The eastern part of Algeria is rich in natural resources like zinc, lead, iron and particularly phosphorite, which have significant strategic and economic importance.

Will outline the geographical location of the study area within its regional context, with a focus on its position relative to major geological structures such as the High Atlas in Morocco and the Tunisian Atlas. This will be followed by a description of the regional and local geology including the stratigraphic succession and the structural characteristics that distinguish the phosphorite-bearing units.

The information is based on previous geological studies (e.g. Kechiched et al., 2016, 2018, 2020; Buccione et al., 2021; Dass-Amiour et al., 2021; Ferhaoui et al.,2022; Laouar et al., 2024, Saouli et al., 2025), in addition to our field observations in the Kef Essnoun area.

1. Regional geology

1.1. Regional geology of atlas saharan

Its a mountain range stretching from west to east, including the Ksour Mountains in s Morocco"s High Atla, followed the Mellegue Mountains in east. Algeria, and the Djebel Amour, Ouled- Nail, Aurès, Hodna, Nememcha-Mezab. It consists of a Mesozoic and Cenozoic sedimentary Layers (e, g., Dubourdieu,1956; Pique et al.,2002). Phosphorite deposits, mainly from the Upper Paleocene and lower Eocene, were deposited in two large basins between newly formed landmasses in this region. The main phosphorite deposits, divided into northern and southern types, are characterized by diverse geological formation, lithological characteristics, and depositional environments. (Kechiched et al., 2016, 2020). The Djebel Onk mining basing, with global-level resources, has been extensively studies geologically by many researchers, such as (Bles and Fleury, 1971; kassatkine et al.,1980; Cielensky et al.,1988; Prian and Cortiel, 1993; Kechiched et al.,2020).

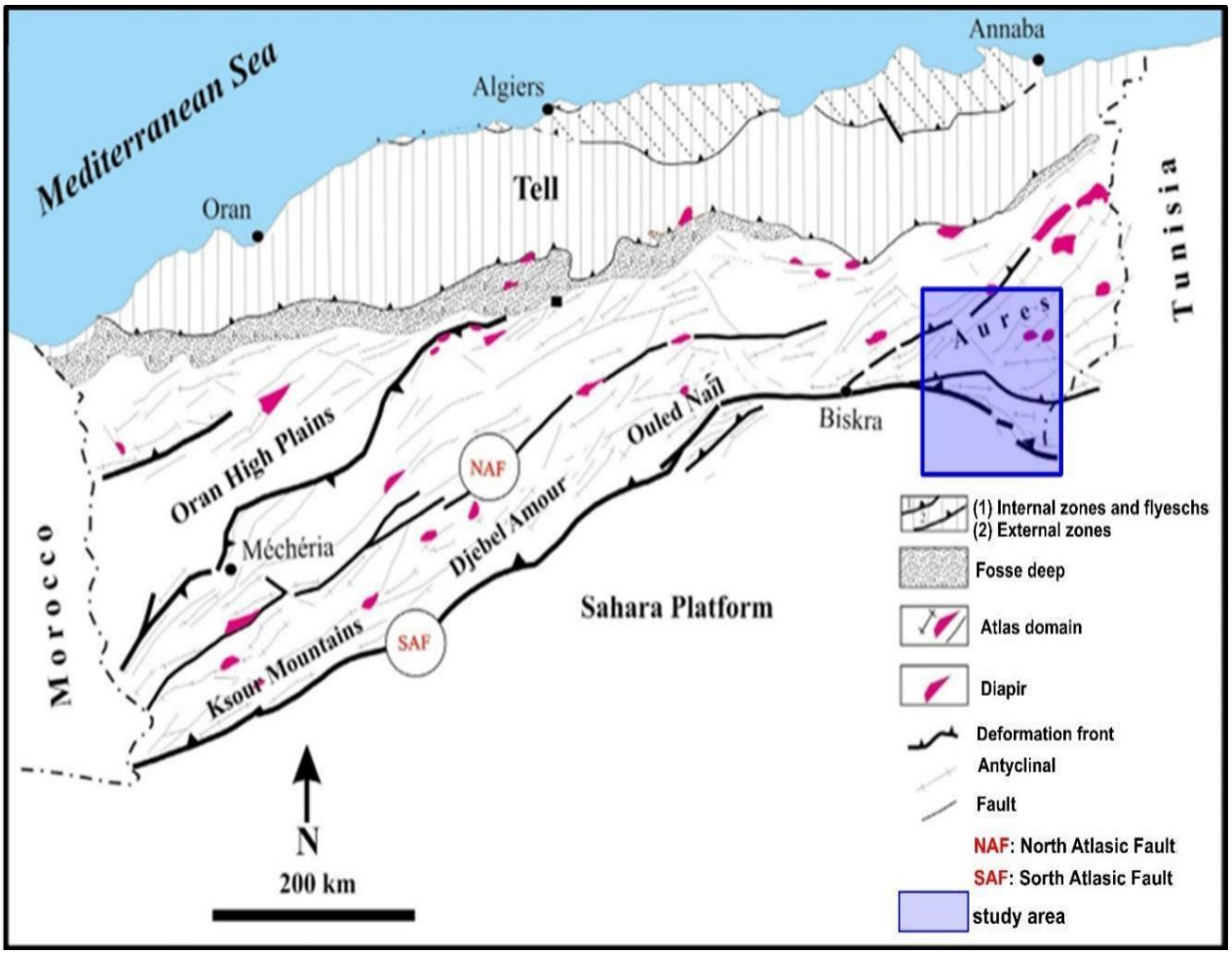

Figure 08: Geological map of Saharan Atlas and area studied.

1.2. Geographic Setting of Djebel Onk

The phosphorite deposits located in the eastern Saharan Atlas constitute one of the most significant mineral resources currently exploited in Algeria. The Tébessa region is particularly notable for is abundant phosphorite reserves, especially in the southern sector of the Djebel Onk area.

This study focuses on the Kef Essenoun mine, situated in the southern part of the Djebel Onk phosphorite basin. The sit lies approximately 100 km from the city of Tébessa, about 21 km from the Algerian-Tunisian border, and nearly 7 km from the town of Bir El Ater.

The kef Essenoun deposit is considered one of the most important phosphorite deposits in Algeria. The phosphorite ore is characterized by Phosphorus pentoxide (P_2O_5) concentrations ranging from 20%to30%, and 2to3.1% Magnesium oxide (Mgo). According to data published in 2024 by the United States Geological Survey (USGS), this deposit accounts for nearly half of Algeria's national phosphate reserves, estimated at approximately 2.2 billion tons.

Exploratory drilling data indicate that the deposit extends over an area of about 2,16 km^2, with an estimated length of approximately 2.7 km and a width of about 0.8 km^2.

The mining basin of Djebel Onk consists of five main phosphate deposits: Djebel Onk North; Djemi-Djema; Belad Hadba ; Oued Bettita ; Kef Essenoun.

The Djebel Onk basin characterized by a semi-desert climate. One of the most prominent climatic phenomena affecting the region is sudden thunderstorms, which lead to rapid and powerful flash floods on the mountain slopes. This causes overflowing wadis and changes in their terrain due to violent water flows. The region is also characterized by scarce rainfall and irregular surface flow of the wadis. The phosphorites in Algeria belong to the phosphogenic province of the Tethys Sea, which developed within two sub-basins: a northern basin and a southern basin, during the period between the Late Cretaceous and the Late Eocene.

At the regional level, northeastern Algeria is part of North African Mediterranean domain, which is characterized by major structural units and a complex tectonic structure (Fig. 9). In this context, the Djebel Onk Basin, located about 80 km southwest of Tébessa, represents one of the most important commercial phosphorite deposits in the world.

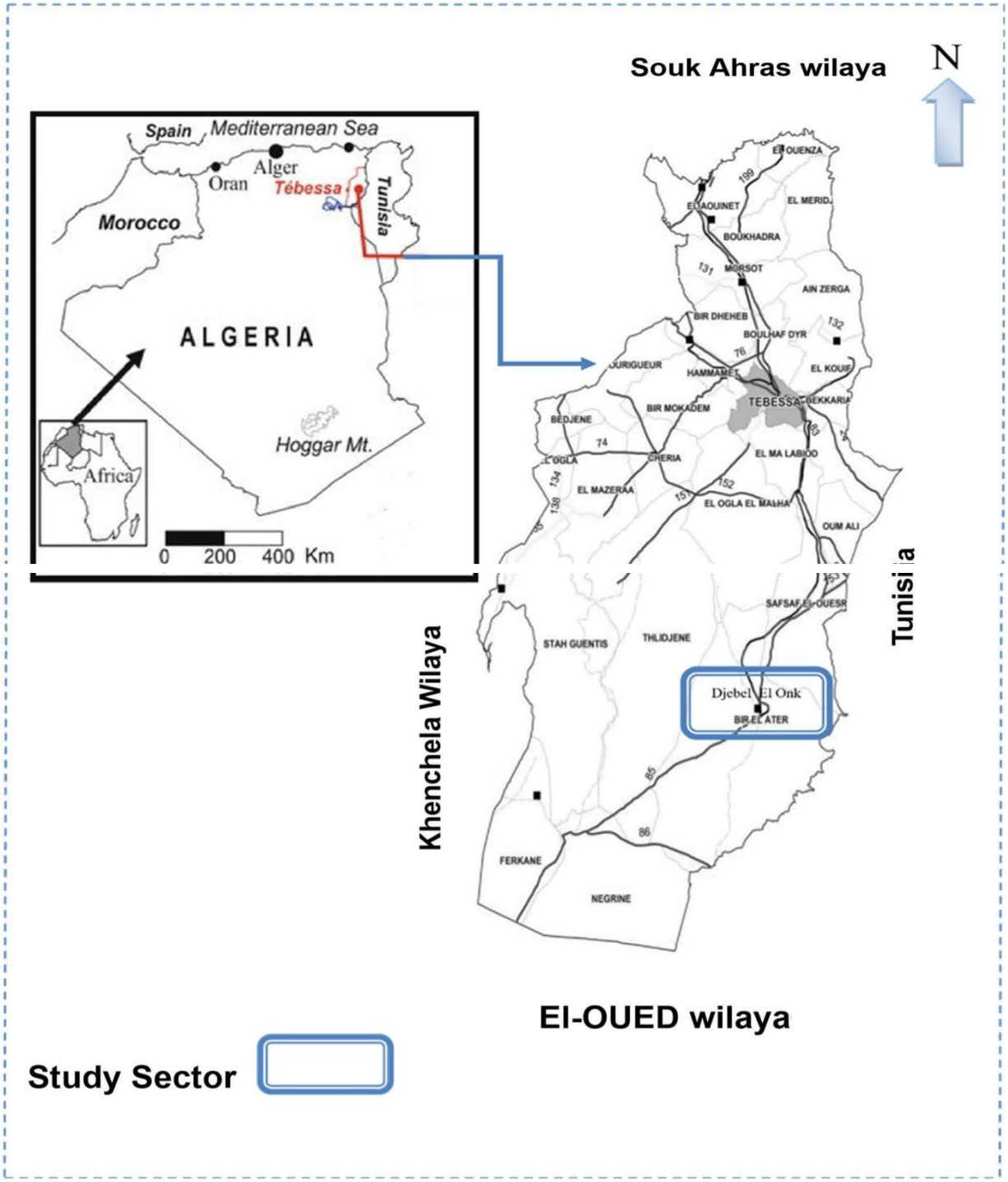

-

Figure 9: Geographical location of the Djebel Onk region

1.2.1. Regional geology of Djebel Onk

The Algerian phosphorite deposits belong to the Tethyan phosphogenic province,wich developed in the northern and southern sub-basins from the Late Cretaceous to the Late Eocene. Northeastern Algeria is part of the Mediterranean-North African tectonic domain and is characterized by several major geological structures (Fig. 10). The Djebel Onk basin, located about 80 km southwest of Tebessa, is one of the most important phosphate basins in Algeria. It contains an estimated 2.2 billion metric tons of phosphate reserves. According to visse (1952), Djebel Onk is an anticline with an Upper Cretaceous core. The basin includes five main phosphate deposits Djemi-Djema, Djebel Onk North, Oued Betita, Bled El Hadba, and Kef Essenoun. Djebel Onk is commonly related to the Gafsa-Metlaoui basin, but its greater subsidence allowed the accumulation of larger phosphate reserves. Its structure is mainly controlled by NW-SE and W-E faults (Visse, 1952).

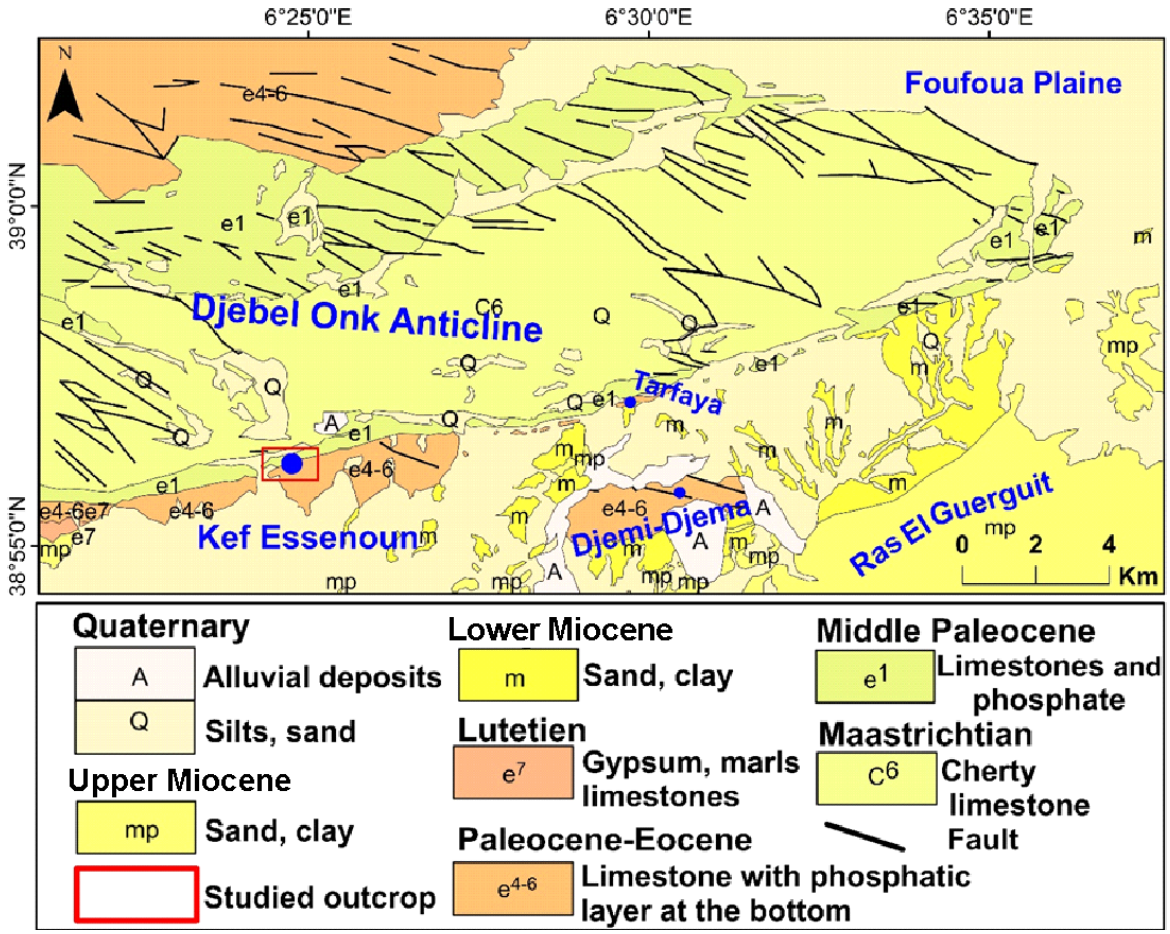

Figure 10: Geological map of the Djebel Onk mining basing (Kef Essenoun), the studied deposit in southern phosphorites (modified after ORGM, 2000).

1.2.2. History of research on the Tebessa region

The discovery of phosphate in Algeria dates back to Ph. Thomas (1855) in the Boghari region. This led to scientific and economic interest in this mineral wealth. Between 1906 and 1907, Joleu discovered the Djebel Onk deposit, the first to identify phosphatic deposits in the area. By the early 1960s, industrialization policies in Algeria prioritized phosphate exploitation. Exploration began in earnest in 1961-1963 with aerial radiometric surveys. Ranchin (1963) continued studies, creating detailed geological map. Actual mining started in 1965 by the Djebel Onk company. Subsequent research and exploration programs were conducted by various organization, including SONAREM and EN FERPHOS, with international collaboration. Studies by researchers like fur (1982), Berats, Kettouche (1970), and Mezghache (1991), contributed to understanding the geology. Visse (1951), estimated reserves at 110 million tons with 24.80 to 25.20% $P2O_5$ Content. Later assessments indicated 600million tons in the Djebel onk area. Further exploration and evaluation programs were undertaken between 1971-1974 and 1985-1987. In 1989, EN FERPHOS announced a development project, and in 1992, a contract was signed with BRGM/SOFREMINs to prepare a development plant for phosphate exploitation in Djebel Onk.

1.2.3. Stratigraphy of Djebel Onk

The stratigraphy of the Djebel Onk region was studied by Visse (1952), and the sedimentary succession exposed in the area is characterized by a stratigraphic sequence extending from the Upper Cretaceous to the Middle Eocene (Lutenian), overlain by a continental series composed of sandy-cly deposits dating to the Miocene and Quaternary (Fig. 11).

1. Cretaceous

The cretaceous represents the oldest deposits exposed in the core of the tectonic anticline of Djebel Onk. Within this period, only the Maastrichtian deposits are present in the area.

- **Upper Cretaceous**

Deposits of this age at Djebel Onk consist mainly of chert-rich limestones interbedded with marl layer. The thickness of this unit ranges between 5 and 10 m. The Upper part of the formation is marked by a weathered horizon with a reddish coloration, forming a level that is easily recognizable in the local topography.

2. Paleogene

These deposits of this stage correspond to marine sediments composed essentially of limestone phosphates, and gypsum. The total thickness of the Paleogene deposits in the region reaches approximately 350 m. Lithological variation and the presence of fossil assemblages have allowed a detailed stratigraphic subdivision of this succession into several stratigraphic units:

- **Danian**

The Danian represents the base of the Paleogene succession. It is defined by the transition between the Maastrichtian limestones and the overlying clayey-marly sequence. This stage is subdivided into two main units:

Lower Danian: This unit consists mainly of marly clay sediments with a dark gray to greenish-brown coloration, interbedded with irregular beds of indurated marls. These deposits are also intersected by gypsum veins with various orientation.

Upper Danian: This unit is characterized by white, fine-grained and compact limestones, often displaying shell-like fractures. These limestones are interbedded with soft clayey marl layers. In the upper part of this stage, a beige limestone bed with a thickness ranging from 1 to 2 m is observed, overlain by withe laminated marls. This level also records the first occurrence of thin phosphatic marl beds, with thicknesses varying between 10 and 30 cm.

- **Selandian:**

The Selandian deposits are characterized by a stratigraphic succession mainly composed of limestones, detrital limestones, and Lumachelles limestones rich in shill fragments, with intercalation of marl and dolomite. These sediments are distinguished by the absence or very low abundance of flint. In addition, oysters are particularly abundant and occur in beds ranging in color from gray to black.

- **Thanetian:**

The Thanetian corresponds to the mineralized horizon and is clearly exposed on the flank of the anticline of Djebel Onk, were it reaches a total thickness of about 72 m. It can be subdivided into two main unit:

Lower Thanetian: This unit is characterized by the presence of marly schists irregularly interbedded with limestone layers. These schists are generally dark gray to black in color. At the base, a conglomeratic level rich in gastropods is observed, followed by thin phosphate layers

and a series of intercalated marls containing characteristic faunal assemblages rich in organic matter. In the upper part of the lower Thanetian, phosphate intercalation reaching up to 2 m in thickness occur and are particularly rich in organic matter. These levels are overlain by limestones and, marl containing large gastropods. The total thickness of this unit varies between 30 and 40 m.

Upper Thanetian: This unit begins with a dolomitic gastropod-bearing level, overlain by a phosphate layer averaging about 30 m in thickness in the regions of djebel Onk and Bled El Hadba. The thickness of this phosphate layer gradually decreases toward the north, west, and south unit it disappears beyond the limits of the deposit. The sequence generally ends with a Lumachelles level rich in shell debris.

The boundary between the Thanetian and the Ypresian is marked a clear transition from phosphate facies to marly limestone facies, with a thickness ranging from 0 to 50m.

3. Eocene

- Ypresian

It rests directly on the Thanetian deposits and outcrops in the Djemi-Djema quarry and nourth of Djebel Onk. Its thickness reaches about 32 m.

Lower Ypresian: At its base, its is represented by conglomerates marking the boundary with the Thanetian deposits. Above them lies an alternation of limestone, marl. And dolomite with a phosphatic layer. Thin flint layers are observed within the limestone. The average thickness of the lower Ypresian reaches about 30 m at maximum.

- **Lutetian**

This stage is divided into two parts:

Lower Lutetian: Characterized by soft white marls containing chert nodules and quartz geodes, replacing the previously dominant limestone, Its thickness ranges between 40 and 50 m.

Upper Lutetian: composed of gypsum, green clay, phosphatic green clay, and limestone forming an evaporitic sequence. The total thickness is about 65 m, including a 10 m layer of phosphatic green clay and limestone at the base, while the upper part consists of green clay interbedded with gypsum. The characteristic fauna includes Cardia placunoides and Ostrea multicostata.

4.Miocene

The Miocene consists of three concordant formations of terrigenous rocks, including conglomerate, clays, sand, and shales:

- **Lower Miocene:** mainly represented by about 200 m of thin siliceous clay layers, sand, and conglomerates.
- **Middle Miocene:** composed mainly of clays, sometimes shales, with interbedded fin-to medium-grained sands, reaching a maximum thickness of about 250m.
- **Upper Miocene:** represented by sandy, clay, and conglomeratic facies with an approximate thickness of 350 m.

5. Quaternary

Quaternary deposits are mainly represented by alluvial (colluvial and deluvial) and fluvial deposits, as well as gravels, boulders, aeolian sand, and slop debris.

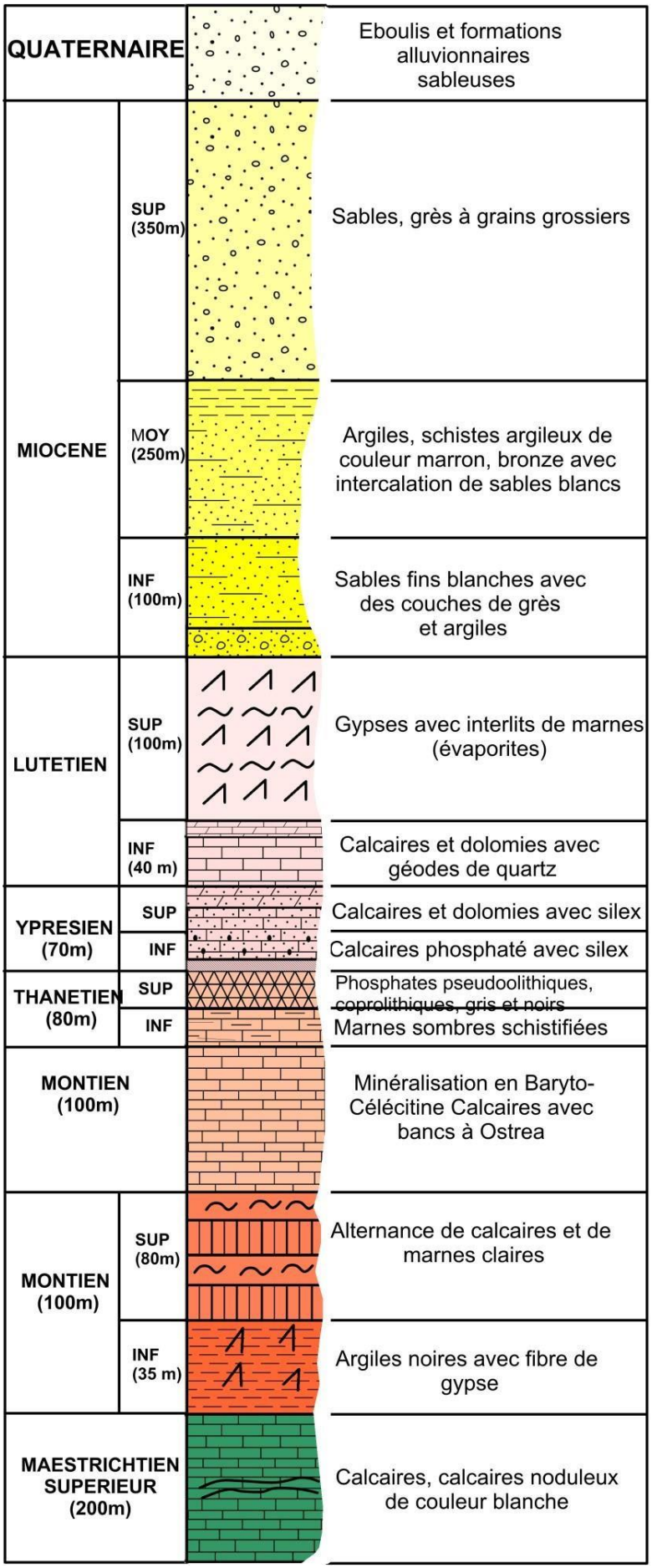

Fgure.11: Djebel Onk region stratigraphic column - Eastern Algeria -(Based on Cielensky and Benchernine, 1987)

1.2.4. Situation structure of Djebel Onk

The eastern margin of the Saharan Atlas from a structural extension that includes the djebel Onk-Gafsa-metlaoui area (Ranchin, 1963). It is characterized by a tectonic structure composed of asymmetrical anticlines and synclines, which are often affected by faulting and disruption along their flanks. These structures generally follow a southwest-northeast (SW-NE) trending axis and are intersected by transverse faults with orientation ranging between N 120° E and N140°E (Fig.12).

The anticline of Djebel Onk represents the principal tectonic structure in the Bir El Ater region. It contains a core of upper Cretaceous age and extends for nearly 20 km along axis oriented N70°E, with an approximate width of 3 km. It was described by Visse (1952) as an asymmetrical anticline resulting from Paleocene tectonic folding. Its southern flank shows a steep dip that locally reaches a sub-vertical attitude, whereas the northern flank is characterized by a gentle dip not exceeding 10°. This northern limb hosts the Djebel Onk phosphate deposit.

About 770m south of the Djebel Onk anticline, whose elevation reaches approximately 1198m at Djebel Tarfata, a lower anticline appears known as the Djebel Djemi-Djema anticline with an elevation of about 883m. The djebel Onk and Djemi-Djema anticline are separated by a collapsed synclinal structure about 1 km wide, filled with detrital deposits dating from the Miocene to the Quaternary (Ranchin,1993., kechiched, 2011) (Fig.12).

The deposits of Bilad El Hadba and Oued Btita occur within a relatively simple structural context, where the sedimentary layers dip at a gentle angle. These deposits belong to the western limbs of Cretaceous-cored anticlines, notably those of Djebel Zerga and Djebel Berki, Djebel Rmetha, which extend eastward into Tunisia within the Metloui rang. In these tow deposits, the strata are affected by disturbances related to transvers faults (Kechiched, 2011).

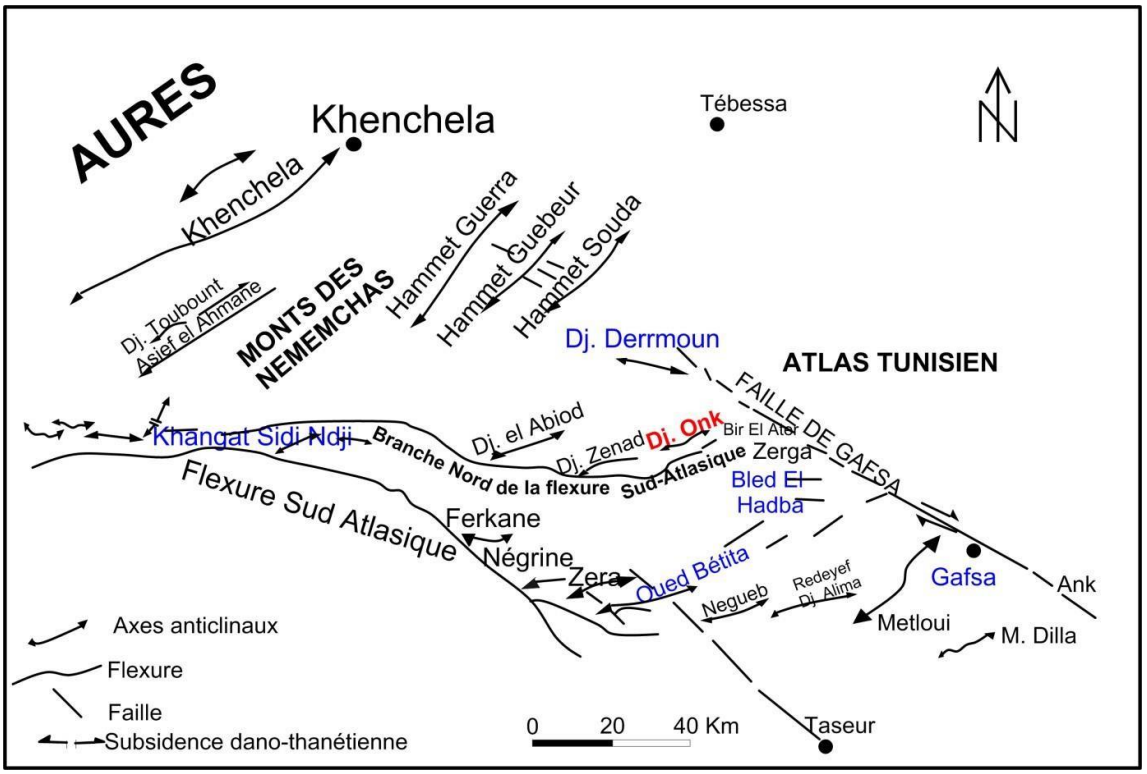

Figure.12: Structural map of the Djebel Onk region within the GAFSA-MUTLAOUI-Onk basin (Aissaoui,1984)

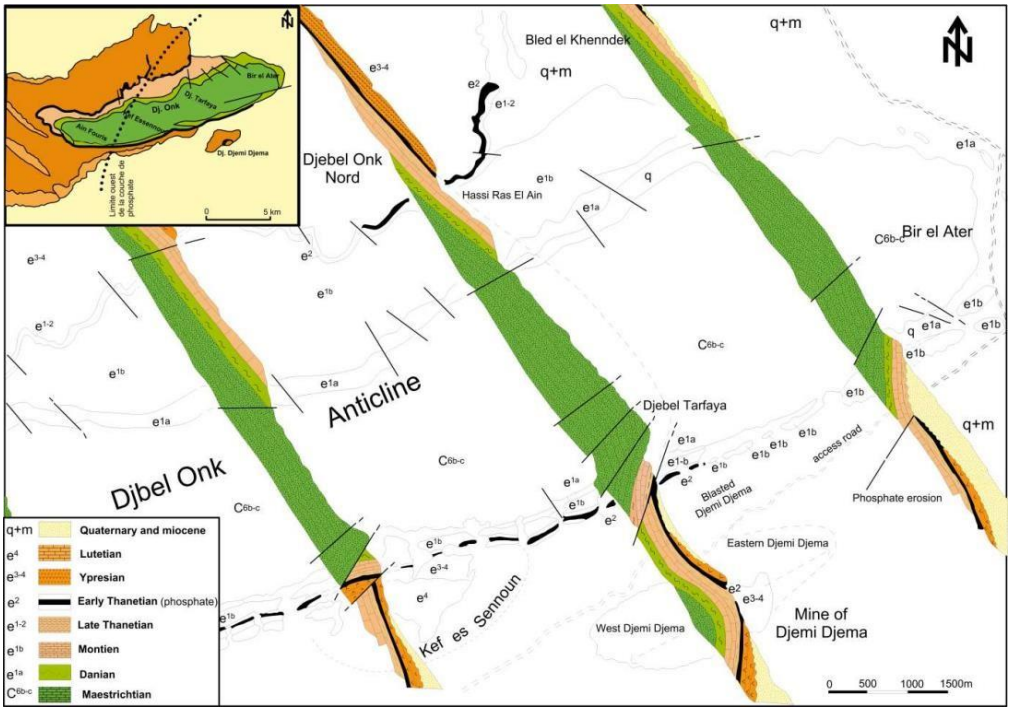

Figure. 13: Stratigraphic and Structural section of the northern and southern flank of djebel Onk (Cielenskyand Benchernine, 1987)

1.2.5. Paleogeography

In northern Algeria, (Sassi, 1980) the end of the Cretaceous period was marked by an important phase of phosphogenesis within the Tethys Ocean. The environmental and marine condition prevailing during this period favored the deposition of phosphate sediments in the Algerian-Tunisian domain around the Kasserine Paleoisland during the Upper Paleocene to Lower Eocene (Kechiched,2018).

Djebel Onk belongs to the western part of the Gafsa-Metlaoui-Onk Basin), the Kasserine Paleoisland is mainly composed of rocks dating from the Upper Cretaceous Period. It is surrounded by three major phosphate basins containing significant phosphate reserves. Among them is the southern basin, which includes the study area and represents one of the most economically important phosphate deposits in Algeria and worldwide, notably including the deposits of Djebel Onk.

The Gafsa-Mutlaoui-Onk Basin is located within a transitional domain separating a highly faulted and folded zone in the north from the relatively stable Saharan platform in the south (e.g, zargouni, 1985; SaId et al.,2011; Garmit et al., 2017).This basin zas supplied by upwelling currents originating from the east through the chotts passage, and it was also in direct connection with the Tethys Ocean to the west (Chaabani,1995).This geographical setting played a fundamental role in the evolution of the sedimentary basin and controlled the depositional dynamics within it.

The sedimentary characteristics of the eastern part of the Gafsa-Metlaoui-Onk Basin indicate deposition in relatively restricted environments controlled by coastal and lagoonal condition. These setting led to the development of a rhythmic sedimentation pattern (Sassi,1974; Chaabani, 1995; Zaier et al., 1998; Ounis et al., 2008). Such condition produced a marked diversity of sedimentary facies, including deposits of chert, clays, carbonates, marl, and gypsum, in addition to phosphates. The ages of these sedimentary facies range from the Cretaceous Period to the Quaternary period.

The first phosphate levels appeared during the Maastrichtian Stage (lower part) within the abiod formation, and later during the lower Thanetian to Ypresian interval within the Chouabine Formation. According to Chabou-Mostefai (1987), based on lithological and micropaleontological data, a clear continuity in the stratigraphic succession has been

demonstrated between the Gafsa-Metlauoui-Djebel Onk basin and its equivalents in Djebel Onk, confirming the unity of the sedimentary and structural framework.

Djebel Onk is characterized by a geological structural related to a structural subsidence phenomenon, controlled by a set of faults trending NW-SE and WE Visse (1952). The Djebel Onk basin contains five phosphate deposits: (Djeme-Djema, Blad El Hadba, Djebel Onk North, Oued Btita and Kef Essenoun).

This basin is composed of a sedimentary succession deposited from the Upper Cretaceous to the Middle Eocene (Lutetian), in addition Quaternary deposits.

2. Local geology

2.1. Geology situation of Kef Essenoun

The Kef Essenoun mine is located within the mining basin of Djebel Onk in southern Tébessa. It lies on the southern flank of the Cretaceous anticline of Djebel Onk. The Kef Essenoun deposit it characterized by relatively simple geological condition, where the phosphorite layers exhibit a gentle southward dip forming a monoclinal structure. The dip of these strata ranges between 10°and 12°.

The topographic elevation of the deposit varies from about 720m in the southwestern part to 810m in the northeastern part. The surface area of the deposit, defined by exploration drilling, is approximately 2.1km^2, extending about 2.7 km in length and 0.8 km in width.

Lithologically, the Kef Essenoun deposit is distinguished by the presence of the main phosphorite-bearing layer of the Djebel Onk basin, wose thickness ranges between 35 and 45m. three superimposed sub-layers (Paraian and Cortiel, 1993) (Figure.14).

- **Basal Layer:** The basal layer consists of two thin phosphorite levels interbedded with marl. The transition toward the overlying main layer may be marked by the presence of a grey dolomite bed approximately 40 cm thick. The thickness of the phosphorite alternation within this layer ranges from 0 to 4 m, with an average thickness of about 1.25. This layer is characterized by a relatively low P_2O_5 content, ranging from 13 to 15%, and a relatively high MgO content, varying between 8 and 10%.
- **Main Layer**: The main layer represents the most important phosphatic level in all the deposits of the Djebel Onk basin. Its thickness ranges between 25 and 30 m and it is mainly composed of phosphorite ores with minor intercalation of marl, limestone, and dolomite

beds. This layer characterized by a high P_2O_5 content and a relatively low MgO content generally (<5%).

- **Upper Layer**: The upper layer is composed of phosphorit with a dolomitic nature. Its thickness varies between 1and 10 m, with an average of about 3 m. This layer is characterized by a relatively low P_2O_5 content (<18 %) and high MgO content ranging from 6 to 11 %. In addition, the SiO_2 content may reach to up 6%. The phosphorite in this layer is generally hard and well consolidated, displaying a dark grey color and a granular texture with heterogeneous grain size, predominantly of coprolitic nature.

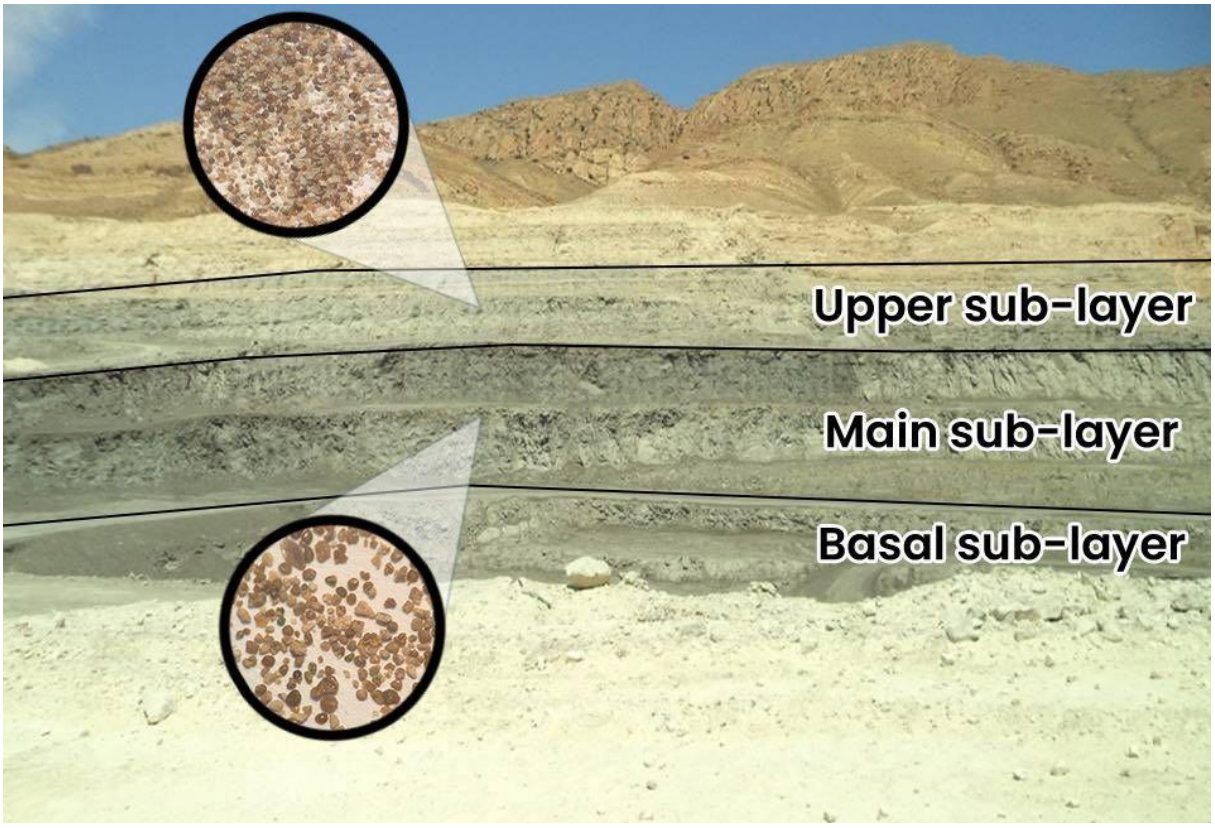

Figure. 14: The Kef Essenoun outcrop (after Kechiched et al. (2020)).

2.2. Stratigraphy of Kef Essenoun

The Mining exploration work carried out by EREM in 1986 made it possible to establish a detailed stratigraphy of the Kef Essenoun (Cielenshy, Benchein,1987), deposit based on a core drilling program organized according to an exploration gride measuring **250 300 m** (Fig.15).

According to the data obtained from the exploration drilling, the entire lithological succession of Djebel Onk is recorded in the kef Essenoun deposit. However, it is distinguished by a notable increase in the thickness of the phosphatic series, with may reach about 53m.

The secondary Formation represent the geological horizon hosting the mineralization and is will developed in the Kef Essenoun deposit (Fig. 15).

1. Cretaceous

The Upper Cretaceous is mainly composed of compact, chalky white limestone and is characterized by the presence of lnoceramus fossils.

2. Paleocene

Paleocene deposits are widely distributed in the region and can be subdivided into several stratigraphic levels as follows:

- Danian

Lower Danian: Consists of greenish-gray clayey marls interbedded with limestone layers.

Upper Danian: Composed of fin-grained chalk alternating with clayey marl layers. It also contains phosphatic levels with decametric thickness.

- Selandian

The deposits consist mainly of limestone containing shell fragments, alternating with marl and dolomite layers. These sediments indicate deposition under variable marine condition.

- Thanetian

This horizon represents the main phosphatic mineralization of the region and shows a well-developed succession, which can be divided into two principal levels:

Lower Thanetian: Composed of dark gray laminated marl interbedded with some limestone layers. The lower part of this unit contains a conglomeratic level rich in gastropods, with the presence of thin phosphatic layers. The upper part includes a phosphorite bed overlain by limestone and marl layers containing large gastropod fossils.

Upper Thanetian: Represents a productive layer forming the main phosphatic material deposited long the southern margins of Djebel Onk. It is characterized by a thickness of about 35 mm which is relatively grater compared to the thickness of other phosphatic layers recorded in the northern deposits (Cielensky et al., 1988;Parian and Cortiel, 1993).

3. Eocene

- Ypresian

Lower Ypresian: Characterized by an alternation of white marl-limestones, marls, and dolomites with the presence of flint nodules in addition to thin phosphatic beds overlying a conglomerate level.

Upper Ypresian: Marked by an alternation of limestone, dolomitic limestone, marl, and phosphatic marl.

- Lutetian

Lower Lutetian: Composed of with calcareous marl and chalky marl containing flint nodules, however, in the upper levels these nodules disappear and are replaced by gypsum.

Upper Lutetian: Consists of alternating light-colored marl and green argillites, which are sometimes phosphatic, with the presence of thin limestone beds and gypsum levels.

4. Miocene

Characterized by continental formations dominated by sandy facies, mainly composed of quartz sands intercalated with clay lenses.

5. Quaternary

Represents the most recent sedimentary formations, characterised by modern alluvial deposits as well as detrital accumulations resulting from slop processes.

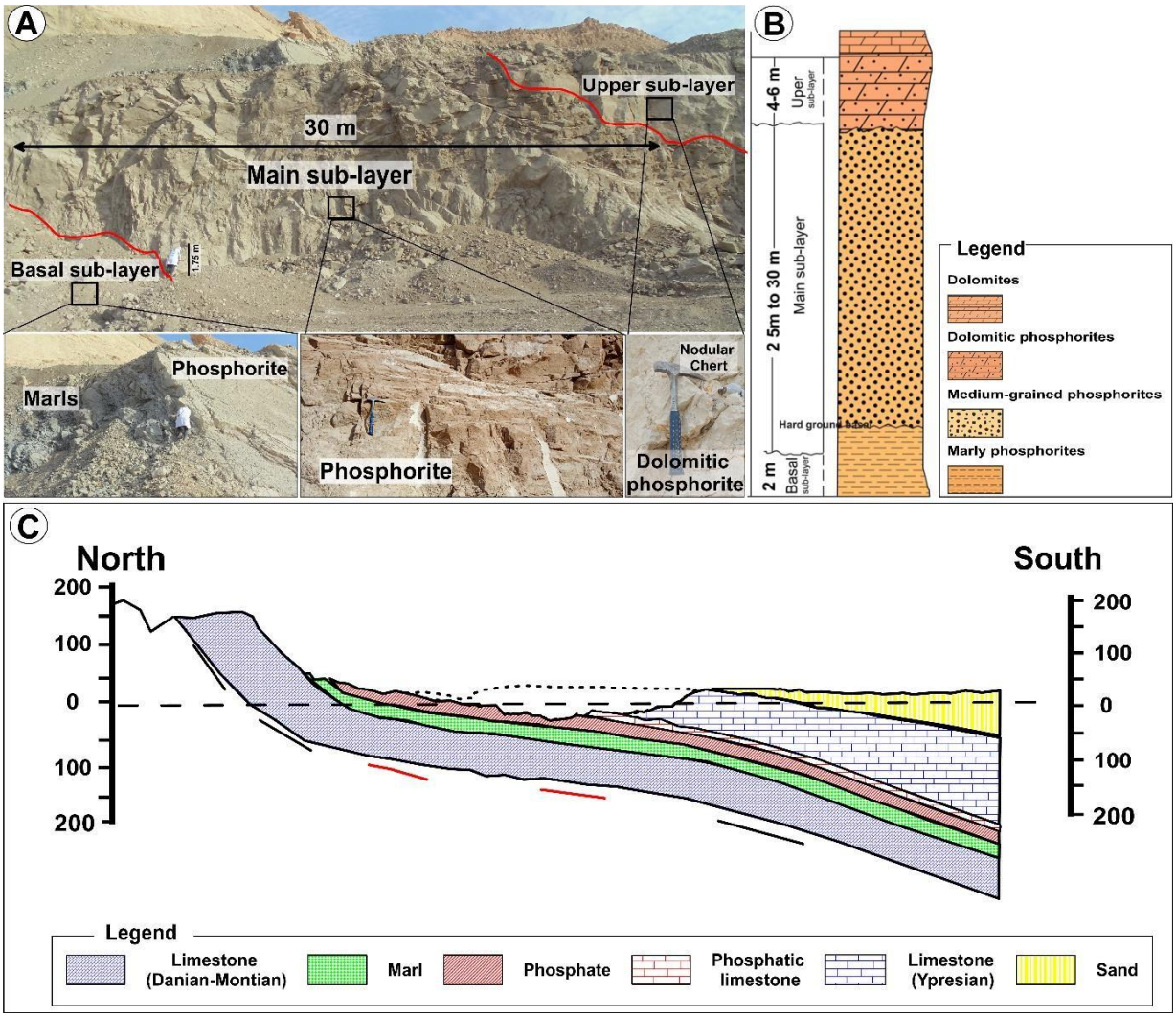

Figure.15: Simplifed lithological of Kef Essenoun deposit (after Saouli (2025))

2.3. Tectonic of Kef Essenoun

Exploration works and studies conducted by EREM revelated that the structure of the Kef Essenoun deposit is relatively simple. The phosphate layers are characterized by a monoclinal dip ranging between 5°and 10° toward the south, with an average thickness of about 30 m. However, observation is the outcrop zone indicate that the structure in this area appears more complex (Dass-Amiour, 2012).

The Kef Essenoun deposit is located on the southern extension of the Djebel Onk antiform flexure, where the main tectonic structure of the region is related to Miocene tectonic movements. In the southern part of the area, a break in slope is observed, where the dip of the layers increases to approximately20°. The deposit is also affected by three major faults trending NNW-SSE, although these faults do not produce significant deformation of the phosphate layer.

In the upright beds zone of Kef Essenoun, which extend in the N75°E direction, the tectonic features become more pronounced. This area is associated with a fractured flexure linked to the overturned limb of the Djebel Onk fold.

2.4. Phosphate of Kef Essenoun

2.4.1 Petrography of phosphate

The petrographic study of phosphate samples collected from the basal, main and upper layer of the Kef Essnoun deposit (South Tébessa) was carried out from both macroscopic and microscopic perspectives.

2.4.2. Petrology

The petrology study of the Kef Essenoun area is not an aesy task, manly due to the difficulty of accessing certain field location. For this reason, samples were collected from the upper layer and the main phosphate layer. After examining these samples using a binocular microscope, several types of phosphate were identified: the main layer, beige and black phosphates were observed, whereas in the upper layer, dolomitic phosphate and black siliceous phosphate were identified. In addition, phosphatic grains with smooth morphology were noted, including coprolites, pellets and glauconite.

A. Beige phosphate

Is characterized by a sandy and friable texture, it contains a carbonate cement, sometimes clayey and is poor in organic matter but rich in phosphatic grain. These grains are relatively uniform in size, with an average diameter of about 0.25 mm (Fig.16).

The pellets and coprolites display rounded and shiny shapes, indicating a certain degree of polishing. This suggests that these particles underwent long-distance transport before deposition, implying a process of reworking or redeposition. As for glauconite, which has a greenish color, its presence indicates a relatively confined depositional environment (Fig.16).

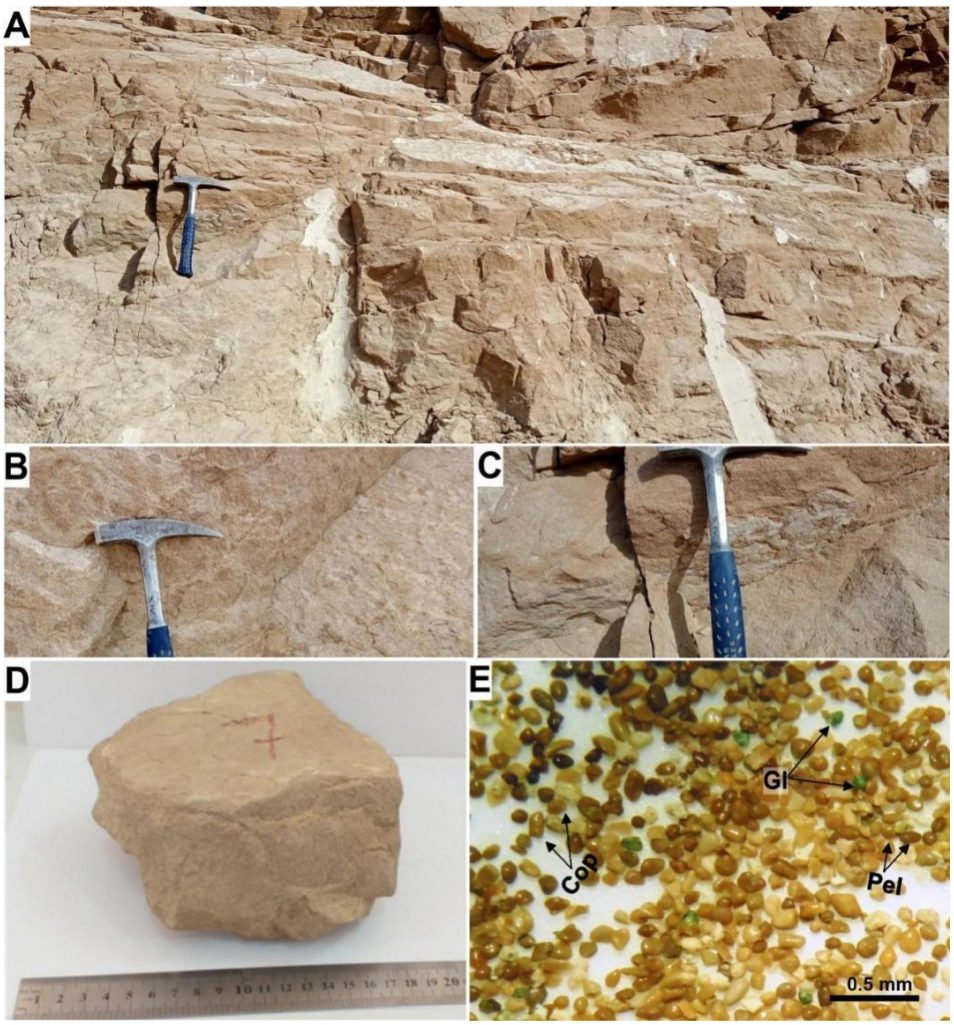

Figure. 16: Beige phosphorite ores from the main layer. (A): Outcrop of beige phosphorite ore the Kef Essenoun quarry. (B): Sample collected from these facies. (C): Phosphatic particles separated from the cement/matrix showing: coprolites, pellets, and glauconite.

B. Black phosphate

Are characterized by a friable outer layer due to the presence of a clayey matrix. This type of phosphate is distinguished by its black colors, indicating a high content of organic matter. Additionally, rounded pellets and coprolites are present, with grain size ranging between 0.2 and 0.3mm. their smooth shapes also suggest prolonged transport before deposition. Fish teeth were also observed within these facies. Furthermore, the presence of green glauconite indicates a relatively high abundance of this mineral in these facies compared to others, suggesting that deposition occurred in a restricted environment (Fig. 17).

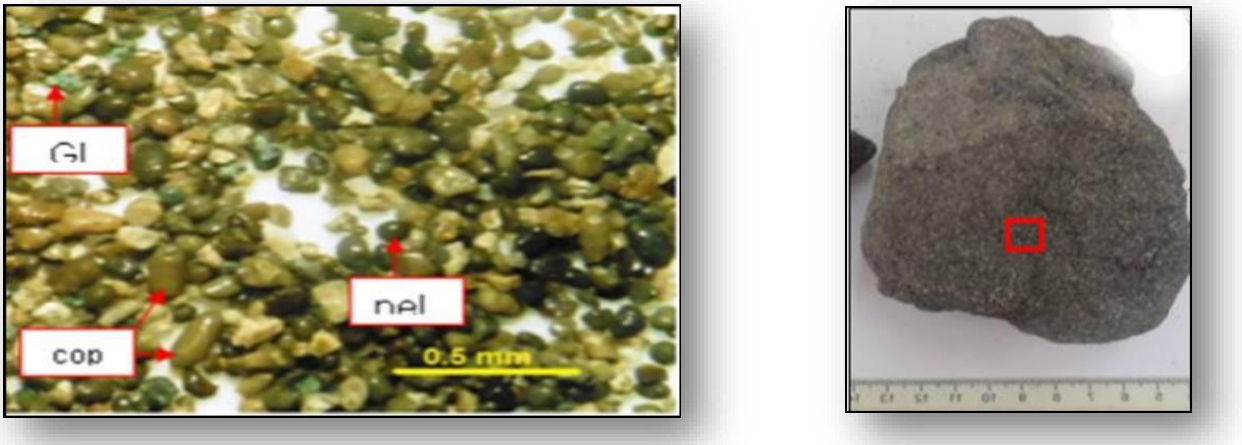

Figure.17: Black phosphorite ores from the main layer. (A) Sample collected from these facies. (B): phosphatic particles separated form the cement/matrix showing: coprolites and pellets, clauconite.

Conclusion

Djebel Onk, the main study area of this work, forms part of the Eastern Saharan Atlas, which extends in a northeast-southwest direction. This geological domain is located approximately 100 km south of the Tebessa region, in northeastern Algeria. The Kef Essenoun phosphate deposits are situated on the southern side of the Cretaceous anticline. The geological structure of the studied area is characterized by a gently inclined monoclinal surface dipping between 5and 10 toward the south. The phosphorite-bearing horizon belongs to the Thanetian stage and reaches a thickness of about 30 metres, reflecting favorable depositional conditions for phosphogenesis and the accumulation of phosphate sediments. Two types of phosphorites can be distinguished including black and beige phopshorites.

CHAPTER 3: PETROGRAPHICL, GRAIN SIZE, AND MINERALOGICAL ANALYSIS

CHAPTER 2: PETROGRAPHICAL, GRAIN SIZE, AND MINERALOGICAL ANALYSIS

Introduction

Sedimentary phosphorite rocks in northeastern Algeria have receive extensive scientific attention regarding their petrographic and mineralogical characteristics (e.g., Sassi, 1974; Chabou-Mostefai, 1987; Kechiched et al., 2018,2020; Boulemia et al., 2021; Dassamiour et al., 2021; Ferhaoui et al.,2022) These studies indicate a notable similarity in petrographic properties across several deposits, especially in Kef Essenoun. These rocks generally contain classic phosphatic components such as coprolites (fossilized feces), pellets, lithoclasts, and bioclasts, which occur within a matrix or cement that varies in nature between calcareous, dolomitic, clayey, or siliceous. These components significantly influence the mechanical properties of the rock, such as its degree of hardness or friability. This chapter aims to study the components of phosphorite in the Kef Essenoun deposit, which belongs to a major phosphate province dating back to the Paleocen-Eocene epochs in northeastern Algeria. Before addressing the geochemical study and its related aspects, petrographic analyses, grain size studies, and mineralogical analyses were conducted in order to provide a comprehensive study of the depositional environments and post-depositional processes that contributed to the formation of phosphorite in the study area.

1. Methodology

1.1. Sampling

As part of this study, field surveys were conducted in collaboration with SOMIPHOS company. During these surveys, a geological cross-section of the Kef Essenoun Phosphate deposit was established. Throughout the fieldwork (Fig.18), a total of 15 rock samples were collected at regular interval ranging between 4 and 5meters.

The sampling was carried out based on the petrographic and stratigraphic characteristic of the different identified units, as follows:

- Samples 0to 5(ech0, ech1, ech2, ech3, ech4, ech5), correspond to marl and basal phosphate layers.
- Samples 6 to 10(ech6.1, ech6.2, ech6.3, ech7, ech8, ech9, ech10), were collection from the main phosphate layers.
- Samples 11 to 13 (ech11, ech12, ech13), correspond to a dolomite layers, which represents a principal phosphate-bearing unit.

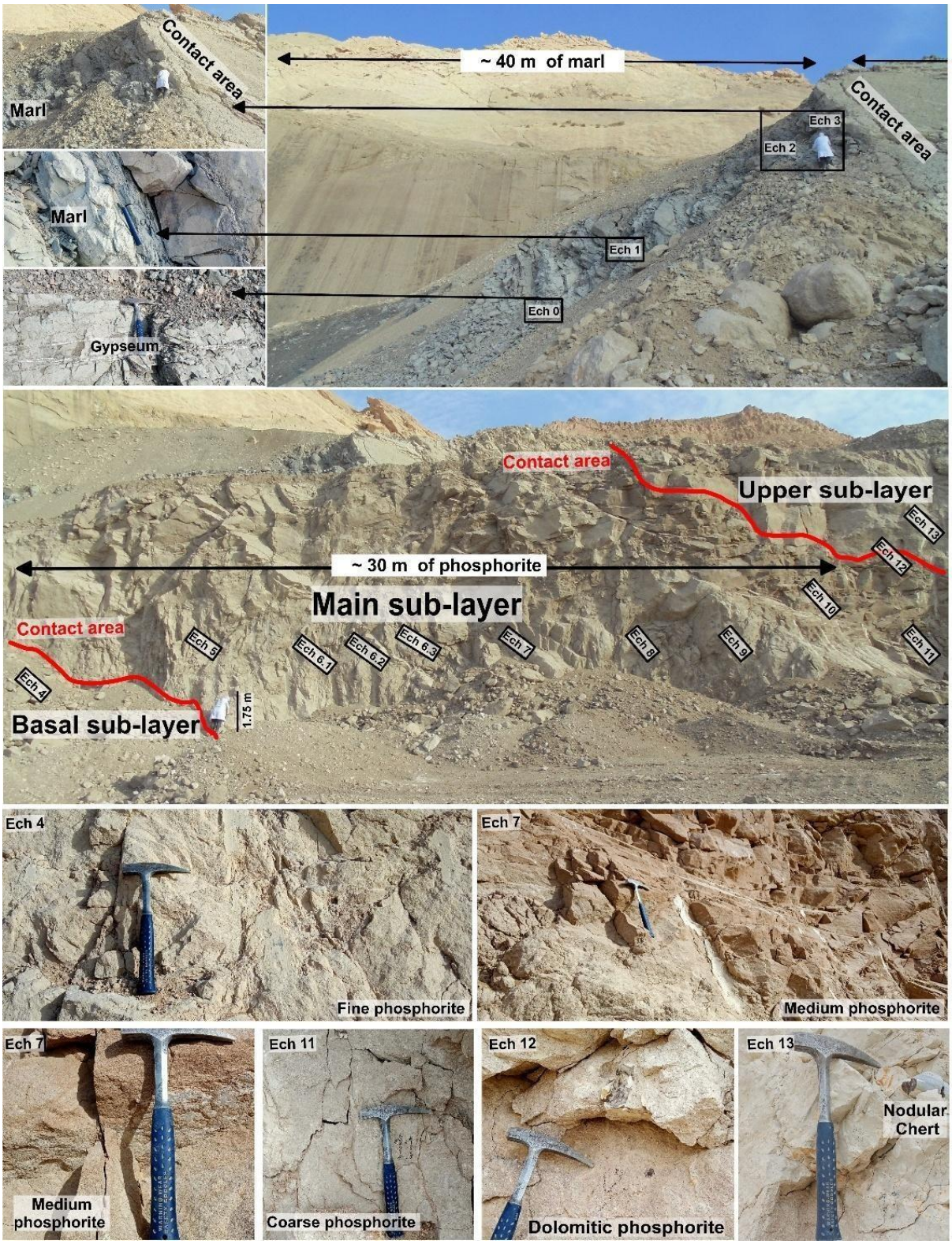

Figure. 18: Field photographs of some sampled phosphorite outcrops in Kef Essenoun deposits (After Safia Saouli 2025).

1.2. Thin section preparation

Preparation of thin section of rocks, one of the most important techniques for studying rocks and minerals under the polarizing microscope. This procedure was carried out at the University of Kasdi Merbah Ourgla, according precise laboratory stages (Fig.25):

- Rock sample selection: seven rock samples were selected from phosphate rocks at Kef Essenoun, Tebessa provice.
- Sample cutting: the samples are cut using saw to obtain small pieces with suitable dimensions of approximately 2*3 cm and thickness of about 1 cm.
- Sample impregnation: because our phosphate samples are friable and porous, they were impregnated with a consoldant (Epoxy Resin) to facilitate cutting during surface levelling. The samples were placed in the resin inside a vacuum chamber for ½ h.
- Surface leveling: one face of the sample is ground on a rotating lap using carborundum powder with graded grain size (220 – 320 – 420 – 600 – 800 µm) to obtain a flat surface that glass slid.
- Grinding the glass slide: the glass slide is ground using carborundum powder with grain sizes (220 - 320 µm), to roughen the glass surface and ensure good adhesion of the sample with the adhesion.
- Mounting the sample on the glass slide: after the adhesion has dried , the upper face of the sample is gradually cut and ground using a lapping machine until the sample thickness reaches 30 µm, the standard thickness that allows light to pass through the mineral.
- Final polishing: final polishing is performed using carborundum powder with a fineness of (600 - 800 µm) to obtain a smooth, scratch-free surface, which improves the quality of observation under the polarizing microscope.

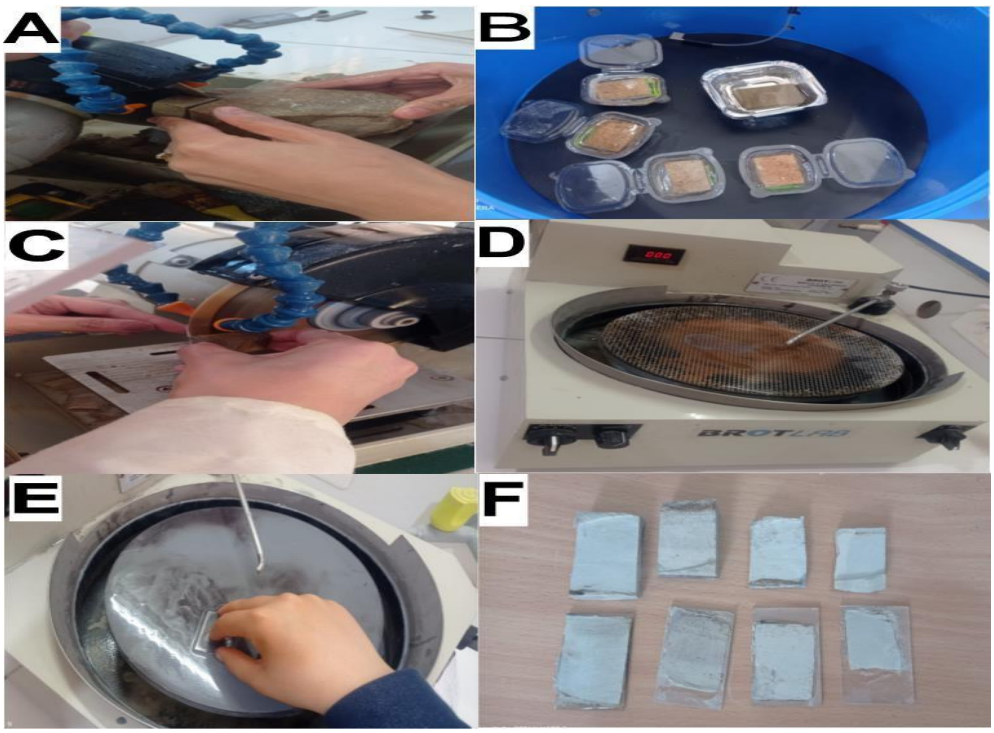

Figure. 19: Preparation of thin sections for phosphorite rocks.

1.3. Petrography

To understand the components of phosphate rocks and their mineral concentrations, a petrographic analysis was conducted on samples representing different levels within the phosphatic layers through two integrated stages. First, a macroscopic examination was performed on the fragments obtained from sieving to identify the coarse components visible to the naked eye using a hand lens and a binocular microscope. Subsequently, a microscopic study was carried out using a polarizing light microscope, allowing a detailed description of the phosphatic grains and their textural and mineralogical characteristics.

1.4. Grain size analysis

1.4.1. Sample preparation

A total of 15 samples were collected for grain size analysis in order to determine their granulometric characteristics. The preparation process included the following steps (Fig. 19).

- Initial crushing of the samples.
- Approximately 20g of each sample was immersed in distilled water for more than 24h to disaggregate the cohesive particles.
- Sieving was then carried out using a set of standard sieves (30µm, 40µm, 80µm, 160µm, 250µm, 500µm, 1mm.
- The samples were air-dried at a temperature of 40 C°.

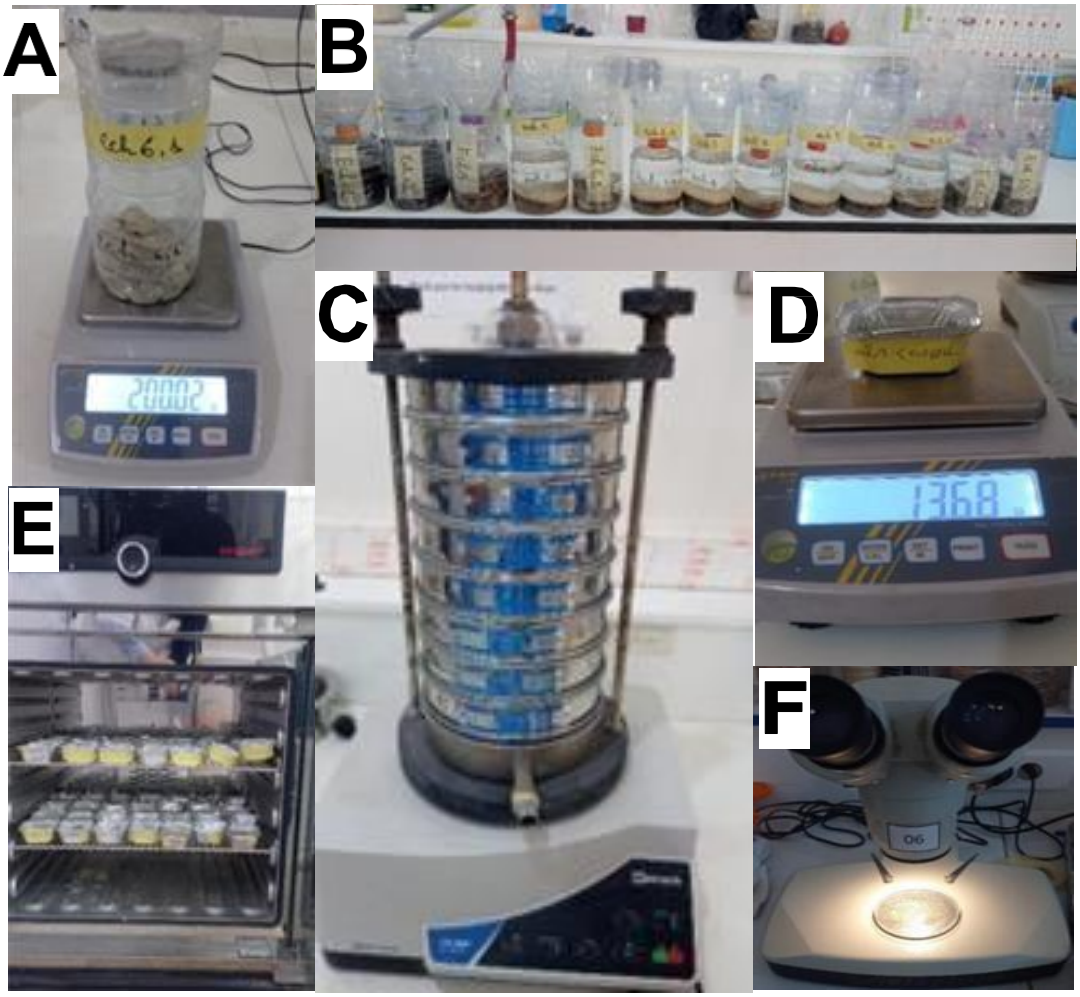

Fig.20: Detailed laboratory processing step from sample preparate.

1.4.2. Methodology grain size data interpretation

Samples were selected from different stratigraphic levels based on their friability and suitability for granulometric analysis. Dry sieving was performed to determine the grain-size distribution and to calculate both relative and cumulative frequency percentages for each size fraction.

The granulometric data were statistically analyzed using the Folk and Ward (1957) method, including the calculation of mean grain size (Mz, Φ), sorting coefficient (σI), skewness (SkI), and kurtosis (KG). Grain-size distribution histograms and cumulative frequency curves were also constructed to facilitate the interpretation of sedimentary processes and depositional conditions.

The analyzed samples were predominantly classified as fine-grained sands, displaying variable degrees of sorting, skewness, and kurtosis. These textural characteristics provide valuable insights into sediment transport mechanisms and depositional dynamics. The

observed granulometric patterns suggest deposition under relatively high-energy conditions, consistent with environments such as beaches, fluvial channels, and shallow marine shelf settings.

All statistical calculations and graphical representations were generated using GRADISTAT software (Simon, 2010). The resulting granulometric parameters were compiled into a summary table (Table 1), enabling comparisons among samples and facilitating the identification of vertical and lateral variations in sedimentary facies and depositional trends.

Table.1: The statistical formulas used for the calculation of grain size parameters (Folk and Ward, 1957).

Grain Size Parameters	Graphical Method (Folk and Ward, 1957)	Interpretation
Mean	Mz = (Ø16 + Ø50 + Ø84) / 3 Ø16: Particle diameter in phi (Ø) units.	
Sorting (Standard Deviation)	σ = ((Ø84 - Ø16) / 4) + ((Ø95 - Ø5) / 6.6) Ø = $-\log_2 D$, where D is grain size in mm.	0 < σ < 0.35: very well sorted 0.35 < σ < 0.50: well, sorted 0.50 < σ < 0.71: moderately well sorted 0.71 < σ < 1.00: moderately sorted 1.00 < σ < 2.00: poorly sorted 2.00 < σ < 4.00: very poorly sorted
Skewness (Asymmetry)	Ski = ((Ø16 – Ø84 + 2×Ø50) / 2(Ø84 – Ø16)) + ((Ø5 + Ø95 – 2×Ø50) / 2(Ø95 – Ø5))	+1.00 > Ski > +0.30: strongly fine-skewed +0.30 > Ski > +0.10: fine-skewed +0.10 > Ski > –0.10: near symmetrical –0.10 > Ski > –0.30: coarse-skewed Ski < –0.30: strongly coarse-skewed
Kurtosis (Peakedness)	KG = (Ø95 – Ø5) / (Ø75 – Ø25)	KG < 0.67: very platykurtic 0.67–0.90: platykurtic 0.90–1.11: mesokurtic 1.11–1.50: leptokurtic 1.50–3.00: very leptokurtic KG > 3.00: extremely leptokurtic

1.5. Mineralogical analysis (X-ray Diffraction _XRD)

To determine the mineralogical composition, X-ray Diffraction (XRD) analysis was carried out at the Saharan Geology Laboratory, University of Kasdi Merbah Ouragla (Fig. 20), following the methodology below:

- In the first stage, a homogeneous powder (<40 µm) was obtained after sieving using standard meshes.
- After preparing the powder; XRD analysis was performed using instrument operating at 40 KV with copper radiation (Ca Ka) at a wavelength of approximately (λ=1.540598 A°).
- Finelly, the obtained diffraction patterns were interpreted using the (ICDD) ASTM database, which contains more than 157000 mineral entries, allowing accurate identification of mineral phases. To interpret the diffraction, patterns, Braggs Law was applied. Each identified mineral exhibition its own characteristic diffraction peak. In addition, manual verification was carried out to ensure that the results matched those automatically provided by the software.

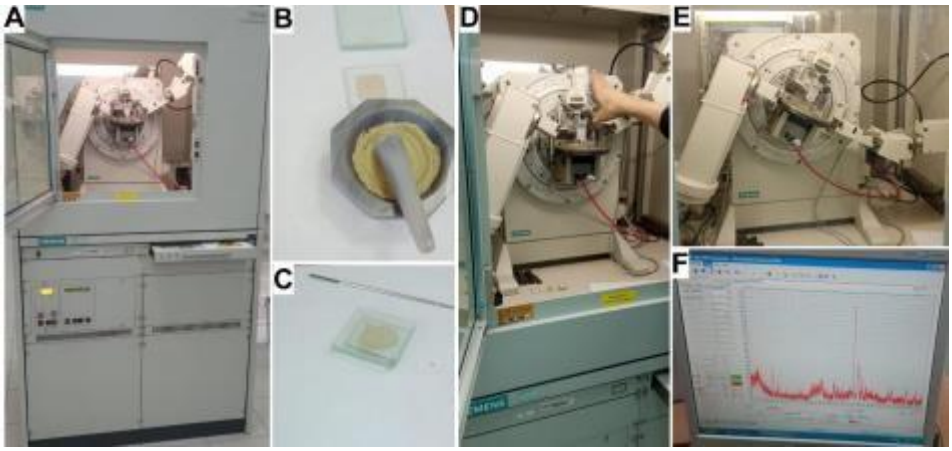

Figure.21: X-Ray Diffraction (XRD) Analysis Workflow: instrumentation, Sample preparation and Data acquisition. (A): Siemens D 500 X-ray diffractometer used for mineralogical analysis. (B): Sample powder placed in a mortar for homogenization prior to mounting, (C): prepared powder sample mounted on a glass slide ready for analysis. (D): Manual positioning of the sample holder.

2. Results

2.1. Petrographic characteristics of phosphatic deposits

A) Pellets

Pellets, under the binocular microscope, appear as spherical grains of varying sizes (250-500 µm), showing noticeable variation in both shape and color. These grains range from cylindrical to rounded forms. They are composed of yellow. Brown, black, and in some cases with components. These rounded pellets are generally considered to have an organic origin, often derived from the fecal matter of small marine organisms. As for the proportion of grain ores, it

varies at each level of the phosphate beds. However, in general, they represent 45% of the total grain components in the ore (Fig. 22).

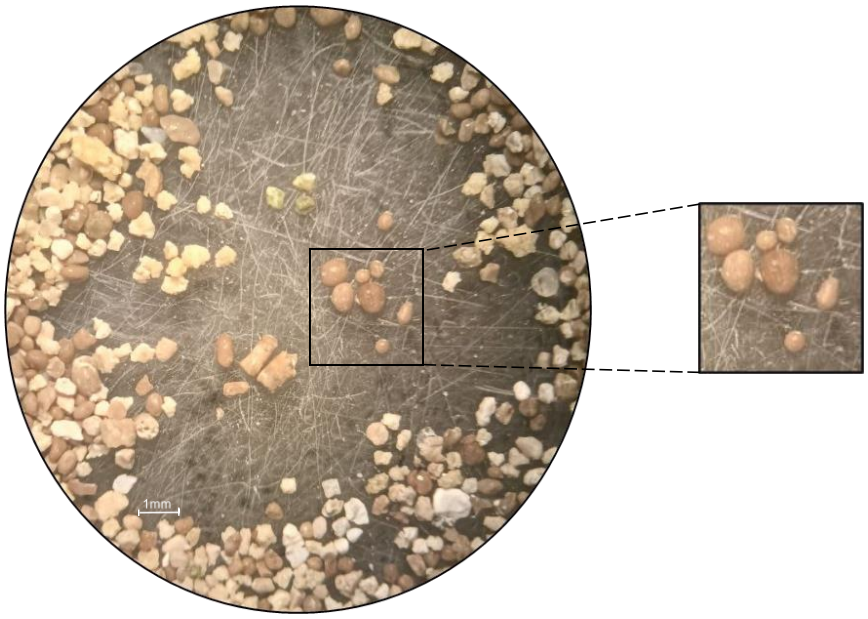

Figure. 22: under binocular observations images showing the morphological and variability of pellets from the studied phosphorites.

b) Coprolites

Coprolites are particles with a cylindrical shape and variable sizes (250-500 µm), they are generally fragile and often fragmented. Coprolite grain are composed of white, yelwo, and brown components (Fig. 23). According to several studies, coprolites are formed from the excrement of living organisms, particularly fish (e.g.,Lamboy et al., 1994). These excrements initially contain phosphatic material, but the phosphorus content is relatively low at the beginning. It subsequently increases through microbial phosphatization processes occurring in oxidizing condition, within confined depositional environments. This diagenetic process is widespread in phosphatic sedimentary deposits. As for the proportion of coprolite grain in phosphorite ores, it varies at each level of the phosphate beds. However, in general they represent 45%of the total grain components in the ore (Fig.23).

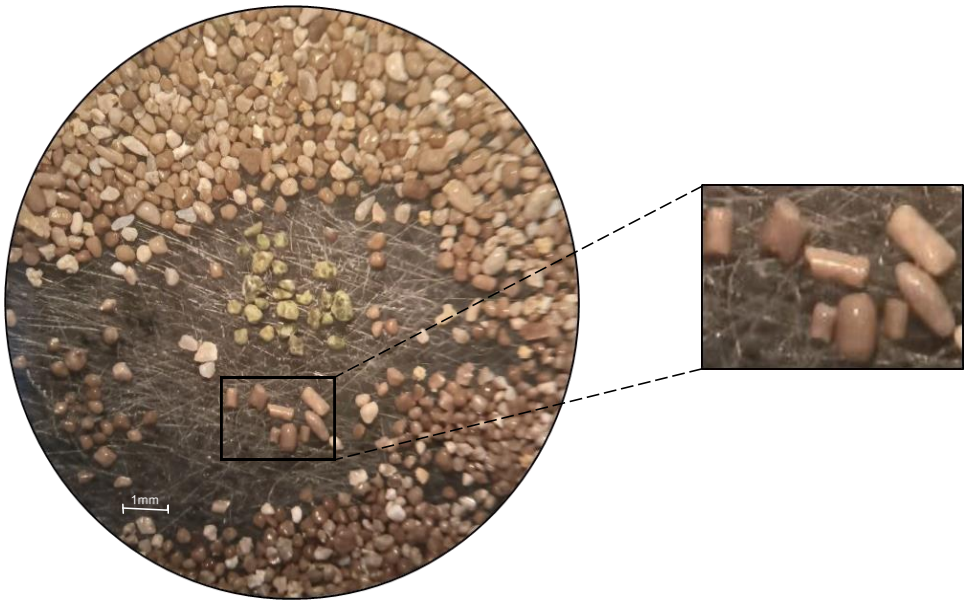

Figure. 23: under binocular observation of Coprolite grains, morphology and internal texter.

c) Glauconite

Glauconite occurs as grains raining in size from a few micrometers to more than 1 mm. These grain may be ovoid in shape. Glauconite is characterized by various shades of green, ranging from light green to pale green, often in its early stages, and from green to dark green in more advanced stages of its formation. Petrographic studies indicate that the proportion of glauconite in phosphorite ores varies between different phosphate layers, however in general they represent 5% of the total grain components in the ore (Fig. 24).

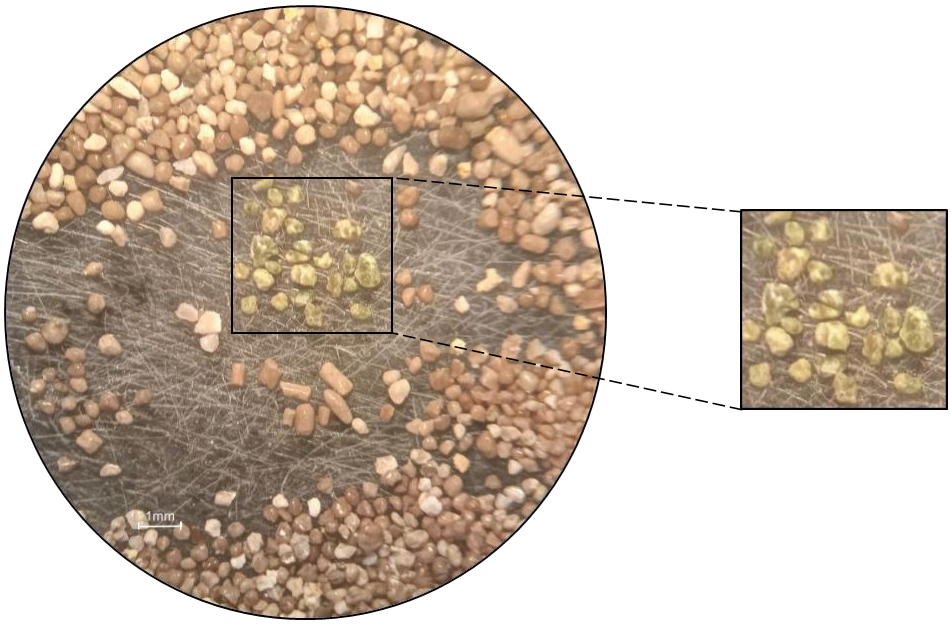

Figure. 24: under binocular observations of Glauconite grains, morphology, and internal texture.

d) Phospho-clastes

The Kef Essenoun phosphate is composed of phosphoclasts formed by the physical fragmentation of lithoclasts and bioclasts. The bioclasts mainly consist of fish bone remains, including well-preserved triangular fish teeth (Fig.25). The Tebessa phosphate deposit is also composed of phosphatized biogenic components (gastropods, bioclasts also include foraminifera, bivalve), (phosphatic grains, according to Kechiched (2017)). As for the proportion of Phospho-clastes grain in phosphorites ores, its varies at each level of the phosphate beds. However, in general they represent 3% of the total grain components in the ore.

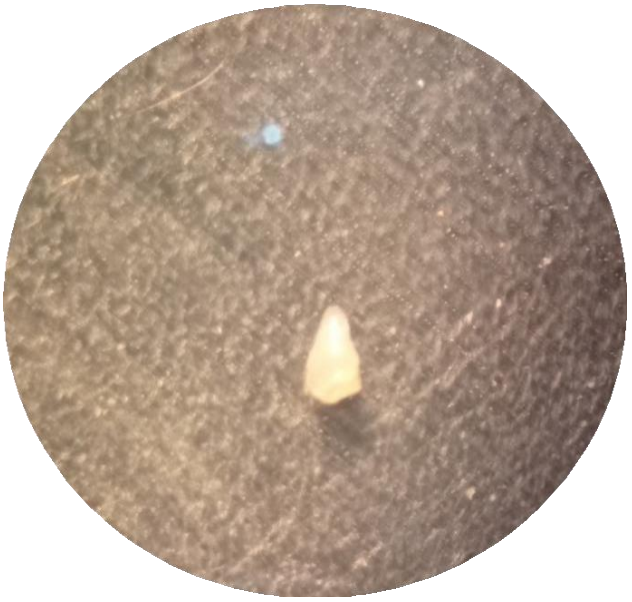

Figure. 25: Under binocular observation of phosphor-classtes (teeth), morphology, and internal texture.

e) Cements and matrices

Phosphatic grains are bound by a cement, which is a crysatalline binding material ranging in size from 5 to 50 µm. It is friable, clay-rich, and black in color, The most common type of cement is typically dolomitic microsparite, with the presence of spiritic calcite. As for the proportion of Cements and matrices grain in phosphorites ores, its varies at each level of the phosphate beds. However, in general they represent 2% of the total grain components is the ore.

Note: In the middle basal layer of the rock, there is a higher amount of glauconite compared to the other phosphate layers.

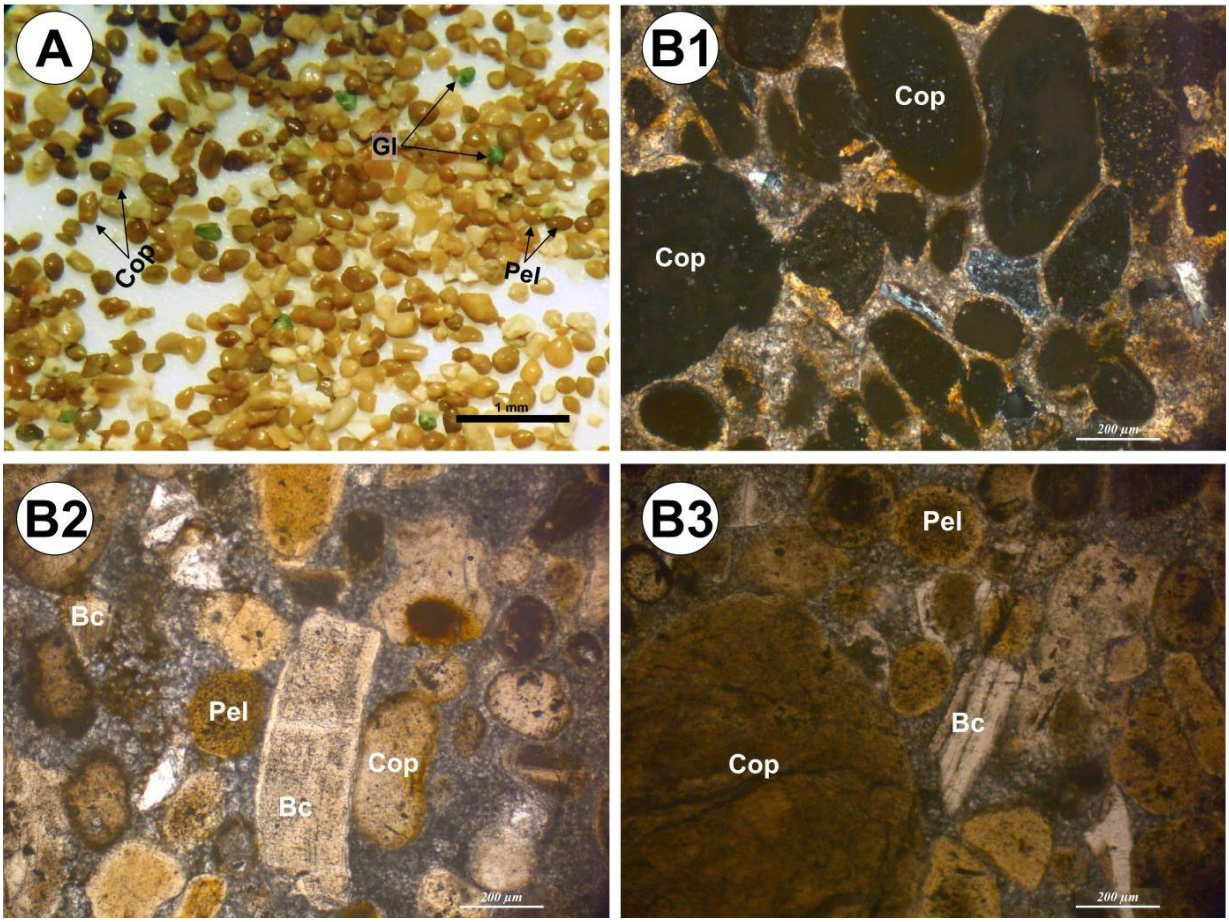

Figure.26: Thin sections under plane-polarized light: (A) pellets, bioclasts and coprolites in clay matrix; (B) pellets and bioclasts cemented by carbonate with iron hydroxides.

2.2. Grain size analysis

2.2.1. Grain size distribution patterns

Analyses were conducted to determine the grain size distribution and particle diameter in phosphorite samples collected from the sub-layers: basal, main, and upper. This was carried out after dry sieving. The grain size distribution was studied to infer the characteristics of the depositional environment (Table .2), represented by relative frequency and cumulative curves as a function of grain diameter.

In the basal sub-layer, which includes sample (ech 5), the relative frequency curve shows that the grain-size distribution is polymodal, with a clear dominance of fin phosphatic particles. A maximum value is recorded at 100 um (28.31%), along with secondary peaks at 80 µm reaching (25.32%). Very low values are observed in the 30-40 µm fraction. In contrast, the coarser fraction (250 µm -500 µm -1000 µm), display very low values, indicating poor sorting and heterogeneity of the sediments.

Table.2: Table of relative frequencies and cumulative frequencies (Unit%).

Diamètre	Frequency	30	40	80	100	160	250	500	1000
Ech 5	Relative	14.37	10.2	25.32	28.31	13.25	5.91	1.07	1.07
	Cumulative	14.37	24.57	49.89	78.2	91.95	97.86	98.93	100

In the **main sub-layer**, which includes samples 6.1,7,8,9 and 10 the relative frequency curve shows that the grain-size distribution is polymodal, with a clear dominance at 160 and 250 µm. There is also a marked decrease in the fine fraction at 40µm and the coarse fraction at 500µm (Table.3). This pattern indicates that the sediments underwent mechanical sorting during transport and deposition, which improved grain selection.

Table.3: Table of relative frequencies and cumulative frequencies (Unit%).

Diamètre	Frequency	30	40	80	100	160	250	500	1000
Ech 6.1	Relative	19.44	6.49	14.75	14.24	21.17	21.73	0.83	1.19
	Cumulative	19.44	25.93	40.68	54.92	76.09	97.82	98.65	100
Ech 7	Relative	6.75	6.85	6.16	8.76	20.06	46.8	2.52	2.06
	Cumulative	6.75	13.6	19.76	28.52	48.58	95.38	97.9	100
Ech 8	Relative	8.99	7.16	9.51	10.19	30.54	27.92	3.64	1.8
	Cumulative	8.99	16.15	25.66	35.85	66.39	94.31	97.95	100
Ech 9	Relative	7.99	5.65	4.91	6.83	45.79	23.26	2.6	2.79
	Cumulative	7.99	13.64	18.55	25.38	71.17	94.43	97.03	100
Ech 10	Relative	7.24	7.26	5.07	12.92	32.42	29.56	2.87	2.61
	Cumulative	7.24	14.5	19.59	32.49	64.91	94.47	97.34	100

In the **upper sub-layer**, represented by sample 11, the highest percentage was recorded at 160µm, around 19-22%, followed by the 250µm and 100µm classes (Tale. 4). This indicates the predominance of medium-sized grains, with a noticeable decrease in the fine fraction at 40µm and the coarse fraction at 500µm.

Table.4: Table of relative frequencies and cumulative frequencies (Unit %).

Diametre	Frequency	30	40	80	100	160	250	500	1000
Ech 11	Relative	13.75	8.87	9.31	14.81	22.19	14.73	8.36	7.95
	Cumelative	13.75	22.62	31.93	46.74	68.93	83.66	92.02	100

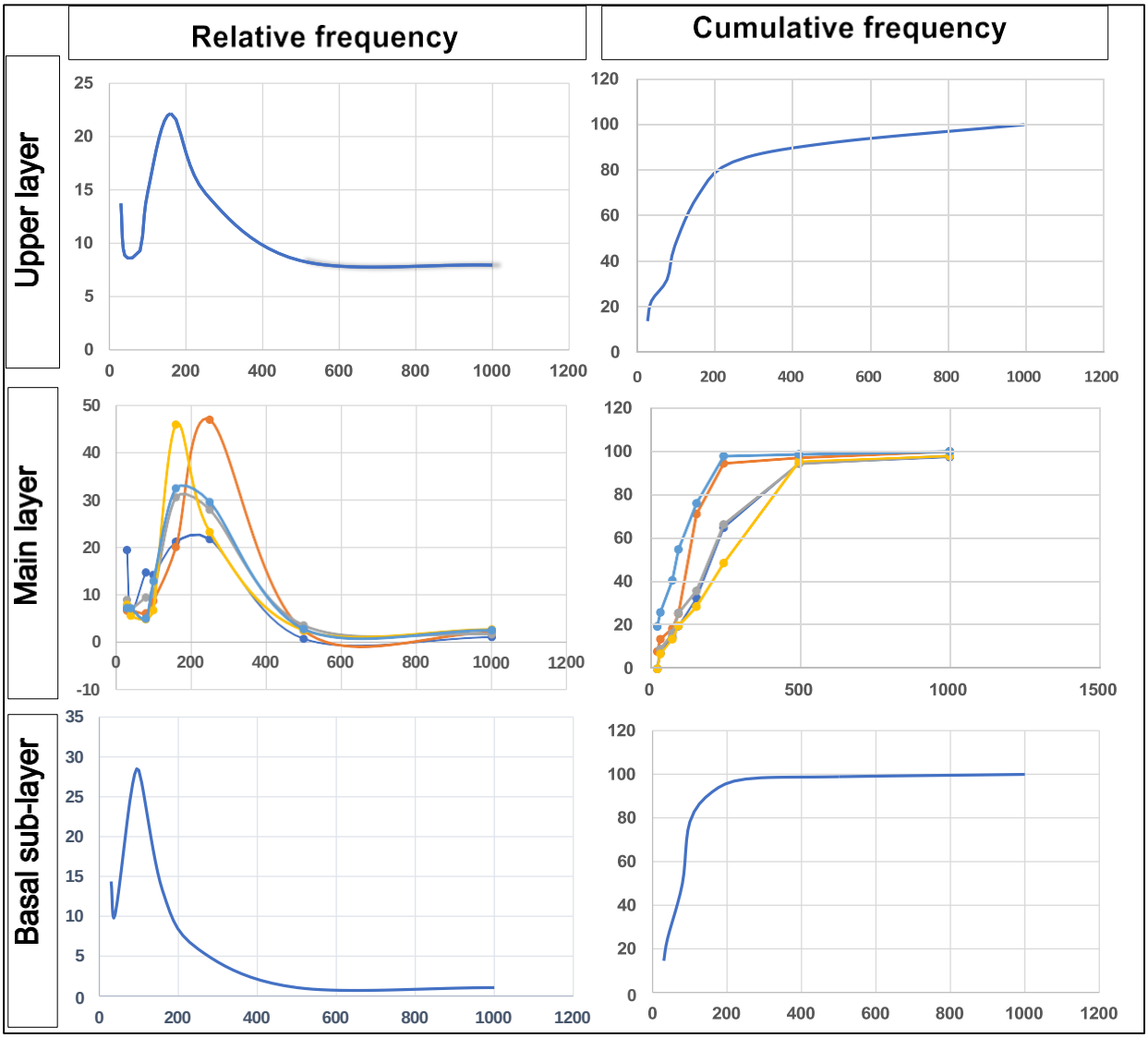

Figure. 27: grain Size distribution of phosphorite Samples from the Basal, Main and Upper sub-Layers: Relative and Cumulative Frequencys.

2.2.2. Statistical grain size parameters

In the Bassal layer (Ech 5), Sorting moderate sorted 1.85 reflects weak mechanical selection and heterogeneous sediment input. Skewness +0.12 indicates a slight enrichment in coarse particles. deposition occurred in relatively high-energy environment close to the sediment source.

In the Main layer (Ech 6.1 to 10), Sorting improves from moderate to very good sorting. Negative skewness reflects enrichment in relatively finer fractions, particulary within the 160 - 250µm rang. Kurtosis > 1, indicates narrow and well-defined grain-size distributions produced by efficient hydrodynamic sorting. The repeated of transport and redeposition contributed to

improving grain selection and sediment homogeneity, which indicates a stable depositional environment.

In the Upper layer (Ech 11), sorting 1.55 moderate will sorted indicates intermediate hydrodynamic condition. Skewness symetrycal suggests a balanced distribution between fine and coarse particles. Based on these results, it is likely that deposition occurred in a calm, low-energy marine environment away from marine currents.

Table.5: Statistical parameters of the results obtained using GRADISTAT software (Simon, 2010). The statistical parameters were calculated based on the method of Folk and Ward (1957).

Layer	Distribution	Main Grain Size (φ)	Sorting (σ)	skewness (SK)	Kurtosis (K)
Basal sub-layer	Monomodal	2.35	1.85 (Moderate Sortes)	+0.12 (Symmetrical)	0.89 (Very platykurtic)
Main sub-layer	Monomodal	2.47	1.4 (Moderate Well sorted)	-0.058 (Fin skewed)	1.11 (Very platykurtic)
Upper sub-layer	Monomodal	2.56	1.55 (Moderate Well sorted)	-0.3 (Symetrical)	1.05 (Very platykurtic)

2.3. Mineralogical analysis

x-ray diffraction (XRD) analysis of the phosphatic succession of the Kef Essenoun mine provided a detailed mineralogical description of the deposits. The succession was divided into three sub-layers: the basal layer, the main layer, and the upper layer, both bulk rock samples and the fine fraction (f< 40 µm) were analyzed (Fig.26), allowing the identification of dominant and secondary mineral phases and the detection of changes related to grain size and diagenetic processes. Results from the bulk rock samples showed the dominance of the apatite phase, particularly carbonate-fluorapatite (CAF), which is the mane mineral constituent of phosphate. This phase exhibited characteristic diffraction peaks at d-spacing, d =2.64, 3.44, 2.79, 2.71A°, confirming its abundance within the phosphatic succession (Chabou-Mostefat, 1987, Gafati et al., 2010) (Fig.26). other apatite phases were also identified, including carbonate-hydroxylapatite and hydroxylapatite ($Ca_5(Po_4)_3OH$). These minerals displayed distinct diffraction patterns reflecting the mineralogical diversity of Paleocene-Eocene phosphorite rocks (Cielensk et al., 1988; Kechiched et al., 2020). In addition to the phosphate phases, the

analyses revealed calcite $(CaCO_3)_2$ through its speacks at d= 3.03, 2.494, 2.281, 2.099, 1.911 and 1.847 A° while dolomite CaMg $(CO_3)_2$ was identified by its reflection at d= 2.900, 2.414, 2.204, 2.078, 2.038, 1.809 A°. Quartz SiO_2 was present both as detrital grain and as a diagenetic cement. Trace amounts of gypsum were also detected, along with clinoptilolite, a zeolite phase identified at d= 2.95 A, which has been reported in similar phosphorite contexts (Chabou-Mustefai, 1987). A comparison between the bulk rock samples and the fine fraction showed clear mineralogical variation. A relative decrease in the intensity of franclite calcite, and dolomite peaks was observed in the fin fraction, alongside a noticeable increase in clay minerals. Glauconite was found in both the basal and main layers. These minerals are generally associated with fine marine sediments, and the presence of glauconite indicates low-energy depositional environments and reducing condition (Bzzi et al., 2002, Kechiched et al., 2020). Oval, the mineralogical characteristics of the Kef Essenoun deposits are consistent with those recorded in Paleocene-Eocene phosphorite formations of northeastern Algeria and adjacent Tunisian bassine, indicating similar depositional conditions and diagenetic histories.

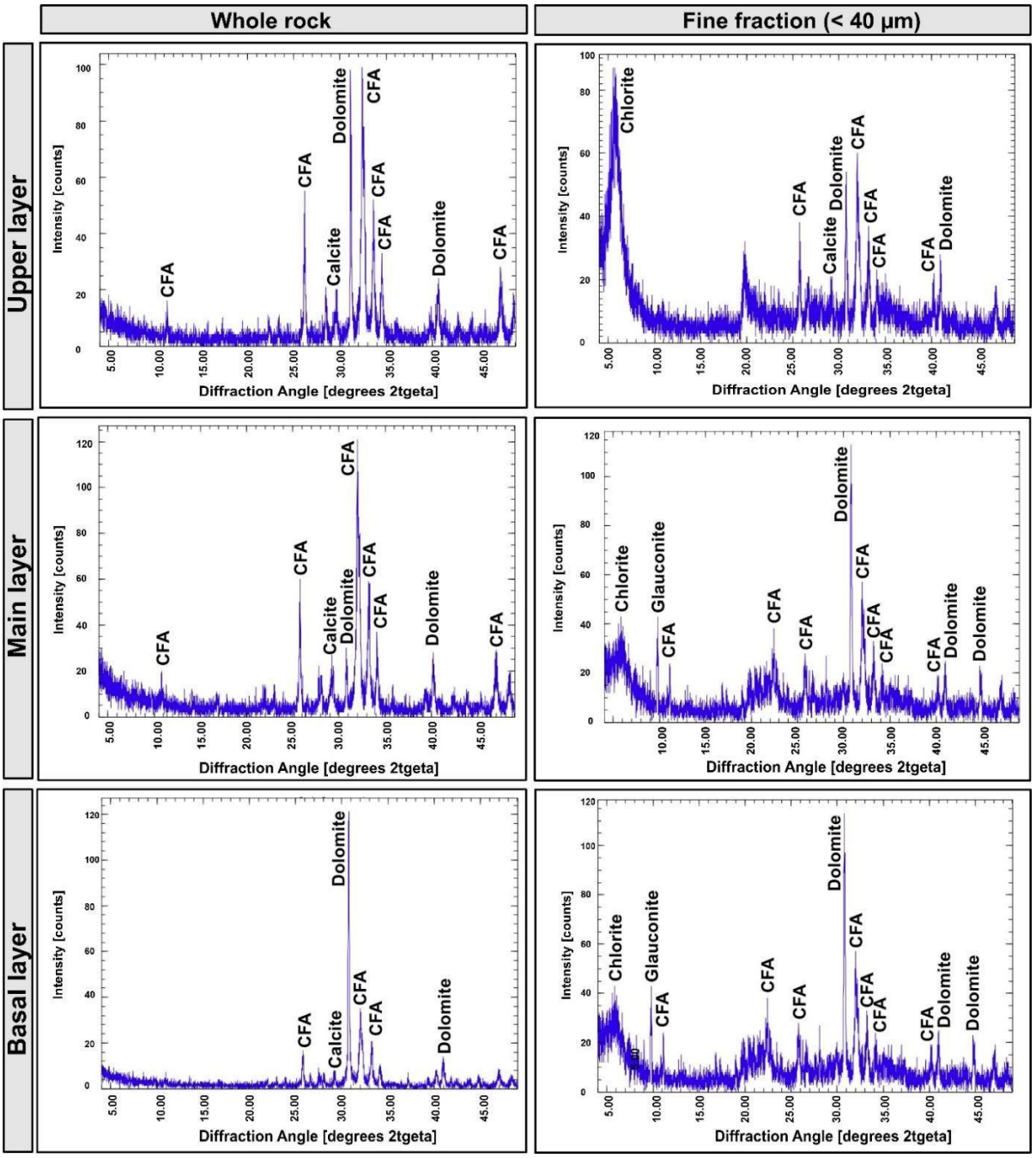

Figure. 28: X-ray Diffraction (XRD) patternes of phosphorite Samples from the Basal, Main, and Upper Lyer, Whole Rock vs Fine Fraction (<40 µm)(after Saouli, 2025).

Conclusion

Based on petrographic analyses, it has found that phosphatic grains and coprolites are among the main components of phosphorite, along with secondary constituents including phosphatic fragments and biogenic remains. These components occur within a micritic to dolomitic matrix, with clear evidence of erosion and reworking processes, in addition to diagenetic transformations such as silicification and dolomitization.

Grain-size analyses revealed multimodal distributions across the phosphatic succession, with clear textural and statistical differences between sub-layers. The basal layer is characterized by poorly sorted sediments with a tendency toward coarse grain sizes, indicating heterogeneous depositional condition. In the main layer, the phosphatic grains are nearly uniform, whereas the upper layer exhibits finer, more uniform, and better-sorted grains, suggesting deposition in a low-energy and hydrodynamically mor stable environment. These results also indicate a gradual evolution from dynamic, proximal depositional environments to calmer and mor stable environments within the stratigraphic succession.

Mineralogical studies based on X-ray diffraction (XRD) technique showed the dominance of carbonate-fluorapatite, along with secondary phases of carbonate-hydroxylapatite and hydroxylapatite. The associated minerals, such as calcite, dolomite, quartz, gypsum, and zeolites, reflect mineralogical variation and the influence of early diagenetic processes.

CHAPTER4:

GEOCHIMECAL AND ENVERONMENTAL IMPLICATION

CHAPTER4: GEOCHIMECAL AND ENVERONMENTAL IMPLICATIONS

Introduction

The phosphorite deposits in the Kef Essenoun area, located in northeastern Algeria, represent one of the most important sedimentary formations with significant economic and geological value in the region. Due to their abundance in phosphorus and their content of a complex suite of trace elements such as U, Cd, Pb, Cu and Z, these elements are known for their potential are toxic effects one environmental systems and human health. These elements can be released during mining, processing, or when phosphate products are used, leading to water and soil contamination. Geochemical studies of these elements are of great importance for understanding the sedimentary processes that have affected phosphate deposits. In this context, this study relies on geochemical approach to describe the distribution of trace and toxic elements within rock samples. To assess the environmental and health impacts related to these elements, this chapter employs at set of geochemical and ecological indices, including the Enrichment Factor (EF), Geo-accumulation index (I-geo), and Potential Ecological Risk Index (PERI). This study aims to understand and identify the source of accumulation of trace and potentially toxic elements within the phosphorite deposits, and to understand the mechanisms
of their distribution and mobility in the sedimentary environment.

1.Sampling stratigy and methodology

1.1. Data and sampling

1.1.1 Samples

The study involves a multi-scale characterization of phosphorite rocks. For whole-rock, six (6) samples from the Kef Essnoun sector of Djebel Onk deposits. Were collected and analysed by (Kechiched et al., 2020), covering various facies such as clayey, marly, calcareous, and siliceous phosphorites.

1.1.2. Analytical techniques

Geochemical analyses of bulk rocks were carried out to determine the concentration of major and trace elements using inductively coupled plasma mass spectrometry (ICP-MS) at the Geosciences laboratory in Montpellier. Approximately 50mg of powdered sample was subjected to acid digestion using a mixture of hydrofluoric acide (HF) and nitric acid (HNO3) on, a hot plate at 110° C for 48 hours. After successive evaporation steps to dryness, the samples were re-dissolved in a 2% nitric acid solution.

This method allows for the precise determination of the concentrations of most major elements, except for SIO2, F, and Loss on lgnition (LOI), which are lost during HF digestion. The

concentrations of trace elements were normalized to the values of the upper continental crust (UCC).

1.2. Normalisation Methodology

To **e**valuate the relative enrichment or depletion of elements, the concentrations measured in whole-rock samples, grain-size fractions, and individual phosphorite particles were normalized to Upper Continental Crust (UCC) reference values according to (Taylor and McLennan, 1985). This normalization approach enables more reliable comparisons between samples by reducing the influence of lithological variability and establishing a geochemical baseline representative of the natural abundance of elements in the Earth is crust. UCC normalization also helps identify anomalies in the distribution of major and trace elements, particularly those of environmental and geochemical importance such as U, Cd, Sr, Zn, Pd, and Cu. The normalized data were illustrated using multi-element bar plots, allowing the recognition of systematic enrichment or depletion trends among different sample types and stratigraphic levels.

1.3. Chemical composition

1.3.1. Major element composition

According to the studies conducted by (Kechiched et al., 2016; 2020), the phosphorites of Kef Essenoun show high concentrations of Calcium Oxide (CaO), exceeding 40 % wt. Meanwhile, phosphorus pentoxide (P_2O_5) is the second most abundant chemical component, with concentration ranging from 18.39%wt to 30.16%wt. In the southern part of the Djebel Onk, represented by Kef Essenoun P_2O_5 concentration range from 27.93%wt to 34.35%wt, with an average of 30.16 ± 2.22%wt. As for MgO concentration, they range from 0.51%wt to 3.21%wt., with an average of 1.73 ± 1.00 % wt. the average P_2O_5/CaO ratio is approximately 1.51± 0.05%wt.

Table. 6: Whole-rock major and trace element contents of phosphorites from Kef Essenoun deposits (data from Kechiched et al., 2020).

Locality	Kef Essenoun (southern deposit)					
Sample no.	S_1	S_2	S_3	S_4	S_5	S_6
Major elements (wt%)						
P_2O_5	30.22	28	27.93	28.98	31.55	34.25
CaO	44.48	43.88	42.84	44.74	46.34	49.85
MgO	1.25	3.21	2.61	2.16	0.66	0.51
Al_2O_3	0.64	0.67	0.9	0.74	0.65	0.07
K_2O	0.18	0.2	0.24	0.26	0.23	0.03
Fe_2O_3	0.51	0.42	0.49	0.46	0.49	0.04
TiO_2	0.031	0.032	0.036	0.028	0.027	0.007
MnO	0.002	0.003	0.003	0.002	0.002	0
CaO/P_2O_5	1.47	1.57	1.53	1.54	1.47	1.46
Trace elements (mg/kg)						
V	67.66	61.93	74.29	71.76	72.57	253
Cr	252	291	285	234	234	290
Li	2.49	2.26	2.64	2.46	2.52	2.03
Sc	2.96	3.85	3.3	2.68	2.64	2.69
Co	0.68	0.58	1.51	0.91	0.77	0.97
Ni	16.86	14.86	17.17	14.59	14.38	39.84
Cu	8.14	8.19	7.71	7.34	7.32	18.37
Zn	169	168	135	107	107	609
As	9.9	10.3	9.79	8.66	9.08	2.79
Rb	4.88	4.54	5.29	4.77	5.03	0.47
Sr	2286	2056	2191	2302	2516	2087
Y	242	305	253	201	222	167
Zr	18.72	23.45	20.07	15.87	16.58	13.15
Nb	0.92	0.99	1.11	0.83	0.8	0.22
Mo	3.19	2.66	3.08	3.05	3.48	3.38
Cd	15.44	24.37	18.08	11.72	11.75	96.88
Cs	2.84	2.67	3	2.6	2.69	0.26
Ba	22.55	19.93	22.71	24.75	25.41	53.39
Hf	0.27	0.35	0.32	0.24	0.25	0.13
Ta	0.09	0.1	0.13	0.09	0.1	0.03
W	0.23	0.29	1.02	0.36	0.33	0.43
Tl	4.49	3.52	3.8	3.43	3.46	0.68
Pb	3.56	4.35	3.65	3.13	3.51	1.76
Th	14.58	22.95	16.72	11.7	12.44	0.81
U	49.2	47.8	48.03	46.03	48.98	76.56

1.4. Relationship between elements and their geochemical associations

stratigraphic level on the concentration of trace elements within the phosphate. Principal Component Analysis (PCA) of the Kef Essenoun samples revealed distinct geochemical clusters related to the stratigraphy position of the samples. It was observed that some samples from Kef Essenoun S-6, located at the Paleocene-Eocene boundary and containing high proportions of Carbonate Fluorapatite (CFA), show high loadings for elements such as CaO, Sr, Y, Cr, P_2O_5,

V, Pb, Ca, Cd, Cu, Zn, these elements are mainly incorporated into the crystal structure of CFA, indicating the influence of this stratigraphic level on the concentration of trace elements within phosphate.

1.4.1. Controlling factors of trace elements in phosphorite rocks

The distribution and concentration of trace metals in phosphorite rocks are controlled by two main geochemical mechanisms play a fundamental role in explaining: substitution and surface adsorption. These two mechanisms play a fundamental role in explaining the geochemical behavior of trace elements and their implication for reconstructing paleoenvironmental conditions.

Substitution mechanisms

The crystal structure of carbonate fluorapatite (CFA)in phosphorite has the ability to incorporate numerous trace metal, especially those with a change and ionic radius similar to calcium (Ca). Among the most important of these elements are: Sr, Li, Nb, Rb, Ta, Hf, and Th. These elements have the capacity to replace calcium within the crystal lattice, leading to their incorporation into the mineral structure (Harouiya et al., 2007; Harouiya and Oelkers, 2004; Rakovan and Reeder, 1996). This substitution is influenced by the prevailing geochemical conditions during phosphorite formation, such as PH, temperature, and the availability of substitution elements. These geochemical parameters can help trace the diagenetic history of phosphate deposits. For example, U, Th, are elements related to changes in redox conditions (Devallois, 2009; Blanchard, 2000;1994, Jarvis et al., Altschuler, 1980).

Surface adsorption mechanism

In addition to substitution, trace metals can also accumulate on the surfaces of phosphorites mineral through adsorption, particularly during the diagenetic transformation phase (Hostar, 1982). This process is controlled by the surface chemical properties of the minerals and environment conditions. Adsorption is a particularly important mechanism for elements such as Mo, As, Pb, Ca Cr, V, due to their affinity for binding to mineral surface (Brown and Parks, 2001), the adsorption process is also affected by several factors, including PH, redox condition and the presence of organic matter.

2. Methodology of calculation

2.1. Environmental assessment indices

The environmental significance of potentially hazardous elements (PHEs) was assessed using indices of assessment risk:

2.1.1. Enrichment factor (EF)

The Enrichment Factor is one of the important geochemical indicators used to assess the degree of enrichment or deposition of chemical elements in sedimentary samples compared to a reference background. In this study the reference background is the Upper Continental Crust (UCC). This index is based on comparing ratio of the concentration of the studied chemical elements to a reference element, such as (Li), in the sample with the same ratio in the reference material. This helps reduce the influence of natural variation related to mineral composition. The enrichment factor is also used to determine the extent to which natural processes affect the distribution and concentration of trace elements in the data (Taylor and McLennan, 1985). The enrichment factor is calculated according to the following equation:

$$EF = \frac{(C/Ti)sample}{(C"/Ti)background} \quad \textbf{(eq1)}$$

Where:

•C: represents the concentration of a particular element in the sample.

•C": background is the concentration of the same element in a background or reference material, often derived from values associated with the Upper Continental Crust (UCC).

The Enrichment Factor is valuable for evaluating the potential impact of human activities on metal

concentrations in environmental samples. It is often categorized into different classes to interpret

the degree of enrichment or depletion. Common classifications include:

•Depletion-to-minimal enrichment: EF < 2

•Moderate enrichment: 2 < EF < 5

•Significant enrichment: 5 < EF < 20

•Very high enrichment: 20 < EF < 40

•Extremely high enrichment: EF > 40

Table.7: Enrichment factor in the elements.

elements	EF1	EF2	EF3	EF4	EF5	EF 6	EF_avg_Ti
V	16.85	14.93	16.17	19.92	21.20	197.56	47.77
Cr	79.03	88.20	78.19	81.61	85.99	284.20	116.20
Li	3.32	2.91	3.07	3.65	3.94	8.48	4.23
Sc	6.07	7.64	5.91	6.12	6.35	17.23	8.22
Co	1.07	0.88	2.07	1.59	1.42	4.77	1.96
Ni	10.21	8.71	9.09	9.85	10.21	75.51	20.60
Cu	8.68	8.45	7.18	8.72	9.15	61.27	17.24
Zn	63.33	61.07	44.24	44.73	47.30	715.77	162.74
As	175.90	177.07	152.00	171.47	189.19	155.36	170.17
Rb	1.16	1.05	1.10	1.26	1.40	0.35	1.05
Sr	174.08	151.52	145.79	195.34	224.69	497.22	231.44
Y	293.53	357.08	267.54	271.39	314.81	633.78	356.36
Zr	2.63	3.18	2.46	2.48	2.73	5.77	3.21
Nb	2.04	2.13	2.15	2.05	2.08	1.50	1.99
Mo	56.68	45.73	47.82	60.39	72.51	187.86	78.50
Cd	4,198.91	6,412.57	4,296.63	3,551.93	3,747.21	82,446.81	17,442.34
Cs	16.45	14.97	15.19	16.79	18.28	4.69	14.39
Ba	1.09	0.93	0.96	1.34	1.44	8.10	2.31
Hf	1.24	1.56	1.28	1.23	1.35	1.94	1.43
Ta	2.40	2.58	3.03	2.67	3.13	2.27	2.68
W	3.06	3.74	11.88	5.35	5.16	18.02	7.87
Tl	159.55	121.03	118.00	135.83	144.18	75.36	125.66
Pb	4.74	5.61	4.25	4.65	5.48	7.36	5.35
Th	36.32	55.31	36.39	32.48	36.34	6.33	33.86
U	468.30	440.22	399.49	488.25	546.71	2,280.29	770.55
V	704.72	6,453.91	10,585.33	3,760.42	21,608.13	5,248.64	8,060.19
Cr	1,463.80	12,127.83	11,614.67	8,462.50	17,321.88	9,062.73	10,008.90
Li	63.66	121.30	93.00	105.00	153.75	79.09	102.63
Sc	26.48	281.74	361.00	150.42	115.00	213.18	191.30
Co	18.45	30.43	23.00	125.83	55.00	21.36	45.68
Ni	403.87	1,398.26	1,864.67	1,385.83	1,106.88	1,452.73	1,268.71
Cu	133.87	984.35	1,464.33	606.67	765.63	1,310.00	877.47
Zn	1,247.11	12,622.17	17,999.33	10,696.25	8,606.25	10,543.64	10,285.79
As	32.75	242.17	268.33	175.42	201.88	426.36	224.48
Rb	65.28	71.30	57.00	72.08	88.75	64.55	69.83
Sr	3,632.61	97,088.26	71,502.00	66,284.17	122,485.00	89,292.73	75,047.46
Y	280.49	10,396.52	12,873.67	8,273.75	9,653.13	11,026.82	8,750.73
Zr	210.70	993.91	748.00	725.00	598.75	691.36	661.29
Nb	40.42	34.35	30.00	38.75	28.75	32.27	34.09
Mo	72.96	33.48	29.33	40.00	60.63	102.27	56.44
Cd	215.56	1,598.70	2,957.33	1,007.50	396.25	1,200.91	1,229.38
Cs	4.58	45.22	31.67	44.58	60.63	4.55	31.87
Ba	291.97	2,237.83	2,598.67	2,305.42	3,500.00	3,784.55	2,453.07
Hf	4.79	12.61	12.33	10.42	7.50	10.91	9.76
Ta	2.68	4.78	3.67	3.33	3.75	2.73	3.49
W	7.75	18.70	13.00	117.50	39.38	11.36	34.61
Tl	21.06	14.78	8.67	96.25	28.13	12.27	30.19
Pb	13.59	79.57	117.00	121.67	83.13	78.64	82.26
Th	13.52	98.70	108.33	72.92	112.50	116.36	87.06
U	80.35	3,942.61	4,200.33	3,294.17	3,823.13	4,796.36	3,356.16

2.1.2. Geo-accumulation Index (I-geo)

The geo-accumulation index is one of the quantitative tools used in environmental geochemistry to assess the degree of pollution or accumulation of chemical elements in sediments and soils compared to their natural background levels. This index provides a quantitative evaluation of the extent of accumulation of a both natural and anthropogenic influences (Meller, 1969). The geo-accumulation index is calculated according to the following to the following equation:

$$I - geo = log2 \frac{Cn}{1.5Bn} \quad \textbf{(eq2)}$$

Where:

Cn: represents the measured concentration of a specific element in the sample.

Bn: is the background or reference concentration of the same element.

The factor 1.5 is introduced to account for potential variations in the background levels.

The I-geo is often classified into different categories to interpret the level of contamination or enrichment:

- I-geo < 0: Practically uncontaminated,
- <0I-geo < 1: Uncontaminated to moderately contaminated,
- < 1I-geo< 2: Moderately contaminated,
- < 2I-geo<3: Moderately to heavily contaminated,
- < 3I-geo < 4: Heavily contaminated,
- geo > 4: Extremely contaminated

2.2. Potential ecological risk index (PERI)

The potential ecological risk index is a measure used in environmental assessments to estimate the potential risks that pollutants, particularly heavy metals, may pose to the ecosystem. The potential ecological risk index is calculated by multiplying the ecological risk factor (Er) by the concentration of each individual pollutant element, as proposed by (Hakansson, 1980). The general equation for calculating the potential ecological risk index can be expressed as follows:

$$PERI = \sum Er = \sum Ti\ (Ci\ sample / C\ background) \quad \textbf{(eq3)}$$

Where:

PERI: is the Potential Ecological Risk Index,

Ti: The toxic response factors were taken according to Hakanson 1980,

Ci: is the present concentration of PHE in the sample,

C: is the present concentration of PHE in the background

Er: consists of the potential ecological risk index for a single PHE.

The ecological risk factor Er is determined based on the potential toxicity and persistence of each pollutant. Typically, a standardized table or set of criteria is used to assign specific values to Er for different pollutants.

The PERI values are categorized to interpret the ecological risk:

PERI < 150: Low ecological risk

150 < PERI < 300: Moderate ecological risk

300 < PERI < 600: Considerable ecological risk

PERI< 600: High ecological risk

The Potential Ecological Risk Index provides a quantitative measure to prioritize pollutants and assess their cumulative impact on the environment. It is a valuable tool in environmental management and decision-making processe.

3. Results and interpretations

3.1. Environmental assessment

3.1.1. Enrichment factor (EF)

The results of the enrichment factor (EF) for potentially hazardous elements (PHEs) in the studied samples,are presented through heatmaps shown in (Fig.28). the results for bulk phosphorite rocks showed very high EF values for Sr, Cd, Y, and U. Cd recorded the highest enrichment levels, with values reaching 49.600. the results also showed that Cr and as are characterized by very high enrichment degrees, ranging from 8 to 170, with an average of 68. Meanwhile, V, Ni, Mo, Tl, Zn, exhibited moderate to high enrichment levels ranging from 5 to 118, with an average of 35. In contrast, low EF values (EF< 2) were recorded for Li, Sc, Pb, Th, Rb, Co, Cs, Cu, Ba, Zr, Nb, Ta, W, Hf, indicating relative depletion of these elements. Samples S-6 was also distinguished by a marked increase in EF values for potentially hazardous elements compared to the other studied samples (Fig. 28).

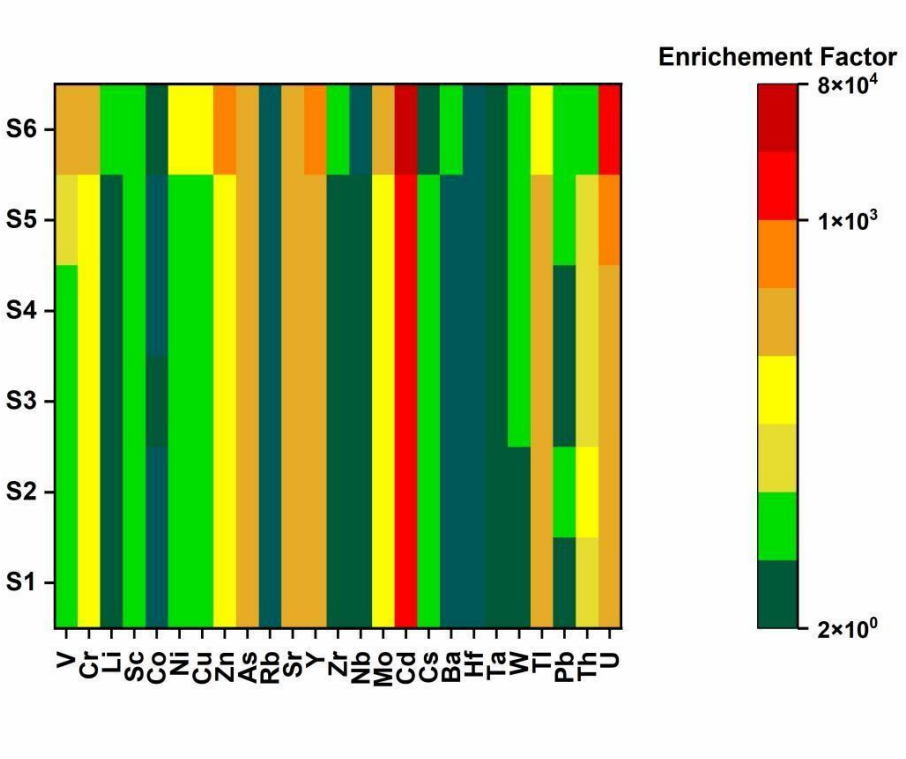

Figure.29: Enrichment Factor heatmaps for whole-rock samples.

3.1.2. Geo-accumulation index (I-geo)

The results showed that the highly potentially hazardous elements exhibited similar behaviour across the different types of samples studied, including bulk rocks, and the various types of particles. (Cd)recorded the highest values of the Geo-accumulation index (I-geo), exceeding a value of (4< I-geo) (Fig.30), while U ranged between (2< I-geo < 4) (fig.29), reflecting ahigh accumulation rate for these two elements.

As, Sr, Y, Re, Cr, and Zn also showed pollution levels ranging from moderate to high, with I-geo values recorded between 2 and 3. In contrast, the I-geo values for L, Sc, V, Ni, Rb, Zr, Cu, Cs, Ba, Hf, Ta, W, Pb, Th, and Mo ranged between (1< I-geo< 2) (Fig. 29), indicating that they fall within the category of practically uncontaminated to moderately contaminated.

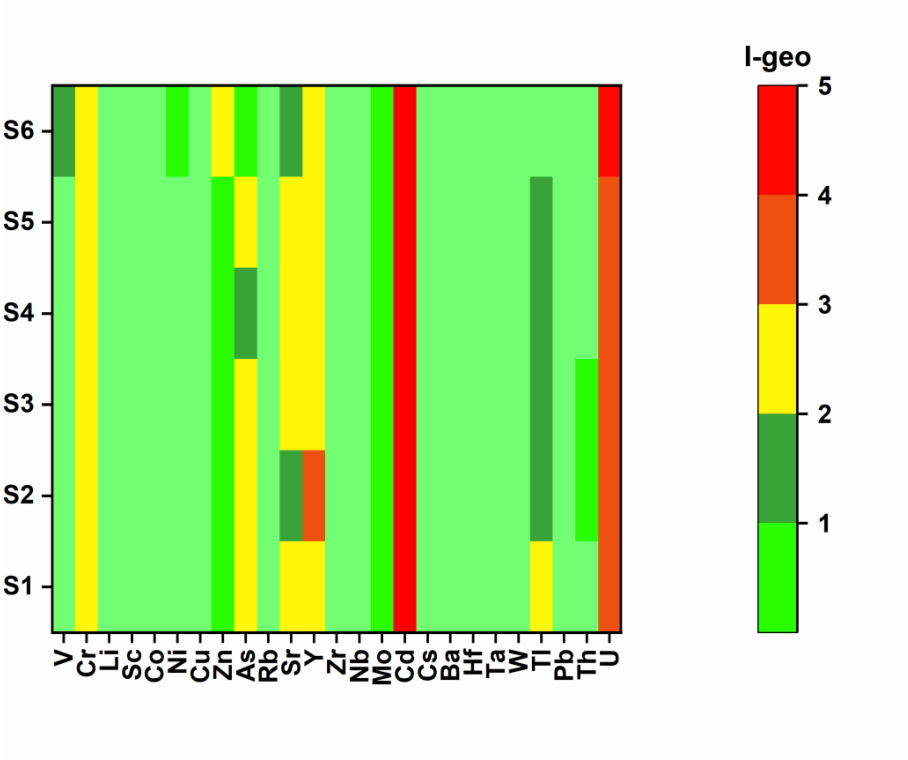

Figure.30. Geo-accumulation index (I-geo) heatmaps for whole-rock samples.

3.1.3. Potential Ecological Risk Index PERI

To evaluate the potential ecological risk associated with potentially hazardous elements (PHEs) in phosphorite rocks, both the individual ecological risk factor (Eri) and the overall potential ecological risk index (RI) were calculated for the different samples, as illustrated in (Fig.30). This assessment was based on the concentration of Be, V, Cr, Co, Ni, Cu, Zn, Cd, Ba, Pb, and U. The obtained results revealed that RI values ranged from 727 to 37,398 across all analyzed samples, indicating a high ecological risk level according to the classification proposed by Hakanson (1980), where RI values exceeding 600 reflect a considerable ecological threat. The

results further demonstrated that Cd was the dominant contributor to the elevated RI values in all simple categories, followed by U and TI. According to the Hakanson 1980 classification, the E^r_i values of Cd fall within the category of very high ecological risk (E^r_i 320), whereas U corresponds to a considerable ecological risk (80 E^r_i 160), and Ti is classified as presenting a moderate ecological risk (40 E^r_i 80). Despite the generally elevated RI values, sample S-6 (Fig.30).

Table.8: Potential Ecological Risk Index (PERI) for the whole-rock, grain-size and particle samples.

Sample no.	V	Cr	Co	Ni	Cu	Zn	As	Cd	Ba	W	Tl	Pb	U	RI
S_1	2.2	4.7	0.1	3.6	5.8	3.3	62.5	8088	0.3	0.3	3.6	0.4	1507	9682
S_2	1.3	5.9	0.2	1.9	1.6	2.4	66	4727	0.1	0.2	59.9	0.9	703	5570
S_3	1.2	6.8	0.2	1.7	1.6	2.4	68.7	7460	0.1	0.3	46.9	1.1	683	8274
S_4	1.4	6.7	0.4	2	1.5	1.9	65.3	5535	0.1	1	50.7	0.9	686	6353
S_5	1.3	5.5	0.3	1.7	1.5	1.5	57.7	3588	0.1	0.4	45.7	0.8	658	4362
S_6	1.4	5.5	0.2	1.6	1.5	1.5	60.5	3597	0.1	0.3	46.1	0.9	700	4416

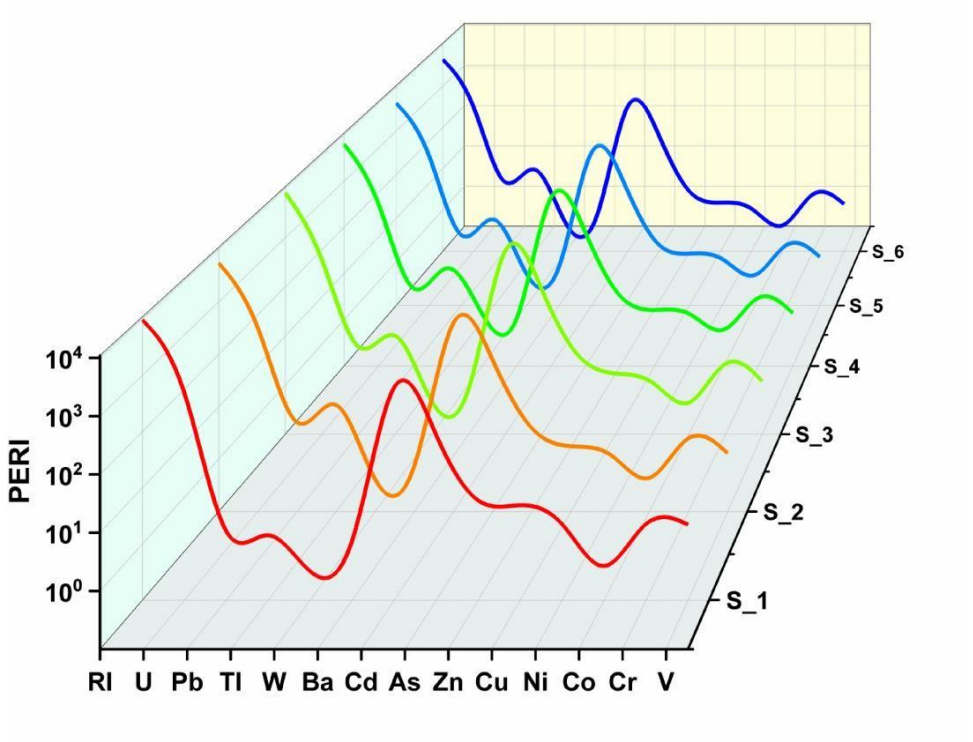

Figure.31: Potential Ecological Risk Index (PERI) for whole-rock.

4. Impact of the depositional environment on the distribution of t (TMEs)

4.1. Relationship between stratigraphic position and the distribution for trace elements and TMEs

Phosphorite deposits are well known for their elevated concentrations of trace elements compared to most other sedimentary rocks, as documented by numerous studies (McKelvey, 1950; Altschuler et al., 1967; Cassa, 1978). The distribution of these elements within phosphorite sequences is controlled by a complex interplay of factors, including stratigraphic position, redox conditions, organic matter accumulation, and biological productivity in the depositional environment.

In the present study, sample S-6, located close to the Paleocene-Eocene boundary, exhibited the highest concentrations of several trace elements and trace metal elements. This enrichment is likely related to the environmental perturbations associated with the Paleocene–Eocene Thermal Maximum (PETM), which occurred approximately 56 Ma ago, as well as preceding warming events (Zachos et al., 1993; Morris et al., 2011; Kocsis et al., 2014; Dong et al., 2024). These climatic disturbances were accompanied by intensified continental weathering, fluctuations in redox conditions, enhanced nutrient supply, and increased marine productivity. Such conditions favored the accumulation and sequestration of redox-sensitive and environmentally significant elements, including U, Mo, V, Fe, Cu, Ni, and Cd, within the phosphogenic sediments. Similar enrichment patterns have been reported in phosphorite deposits from Egypt (Khozem et al., 2015), supporting the interpretation that global paleoenvironmental changes exerted a significant influence on trace element incorporation into phosphorites.

The geochemical and environmental assessment of the phosphorite deposits from the Tébessa region revealed substantial enrichment of certain potentially hazardous trace elements, particularly Cd and U, within the whole-rock samples. The Enrichment Factor (EF), Geo-accumulation Index (Igeo), and Potential Ecological Risk Index (PERI) collectively demonstrated significant spatial and stratigraphic variability in trace element distribution. Among the analyzed samples, S-6 consistently recorded the highest enrichment factors, geo-accumulation levels, and ecological risk values.

Furthermore, PERI results indicated that all investigated samples fall within the high ecological risk category, highlighting the environmental significance of trace element accumulation in these phosphorites. Cadmium was identified as the dominant contributor to the overall ecological risk, followed by uranium and thorium. These findings suggest that the studied phosphorite deposits, particularly those from the Kef Essenoun deposit, may represent a

potential source of trace metal contamination if mining and beneficiation activities are not carefully managed. Consequently, selective extraction strategies and appropriate waste-management practices should be implemented, taking into account the mineralogical hosts and spatial distribution of trace elements, in order to minimize potential environmental impacts and promote the sustainable exploitation of phosphate resources.

Conclusion

A comprehensive analysis of the chemical composition of phosphorite rocks from Kef Essennoun and the variations arising from depositional conditions and diagenetic transformations revealed that whole-rock analyses showed high concentrations of CaO and P_2O_5 which are key indicator of the economic value of phosphorite. Variations were also recorded in the concentration of MgO, Al_2O_3, and Fe_2O_3, reflecting mineralogical differences among the sub-layer. The integrated assessment of environmental and health risks associated with Kef Essenoun phosphorite indicates the presence of high enrichment levels of Whole-rock trace elements, particularly Cd, U, Cr, across the different sample types studied, Cd, recorded the highest enrichment factor, with an enrichment factor (EF) of approximately 49.600. The geoaccumulation index (I-geo) represents an efective and relable tool for assessing polution levels and the accumulation for chemical elements in sediments and soil, morever this index provides a precis quantitative assessement of the degree of metal contamination.It was also the elements that contributed to the most elevated values of the Potential Ecological Risk Index (PERI), as the total Risk Index (RI) exceeded 37.000, classifying these deposits within the category of very high ecological risk.It can be said that the high concentrations of trace elements and heavy metals, especially cadmium and uranium, are the result of climatic and environmental effects associated with the Paleocene-Eocene Thermal Maximum period (PETM).

CONCLUSION GENERAL

The Djebel Onk region, located within the Eastern Saharan Atlas of Algeria, represents one of the most important phosphate basins of economic and geological significance. This study focused on the Kef Essenoun phosphate deposits situated on the southern flank of the Cretaceous anticline. The results revealed that the phosphate formation dates back to the Thanetian age and reaches a thickness of approximately 30 meters, reflecting favorable depositional conditions for the formation and accumulation of phosphate deposits.The petrographic study highlighted the presence of two main phosphate types: black phosphate and beige phosphate. It also showed that phosphatic grains and coprolites constitute the principal components of the phosphatic rock, together with bioclastic remains and phosphatic fragments embedded within a micritic to dolomitic matrix. The findings further revealed clear evidence of erosion and redeposition processes, in addition to diagenetic alterations such as silicification and dolomitization. Grain-size analyses demonstrated a marked variation among the sublayers. The basal layer is characterized by coarse and poorly sorted grains, indicating dynamic and unstable depositional conditions, whereas the upper layers exhibit finer, more homogeneous, and better-sorted grains, suggesting a calm and hydrodynamically stable depositional environment. This evolution reflects a gradual transition from high-energy to low-energy depositional settings throughout the stratigraphic sequence. The mineralogical study based on X-ray diffraction (XRD) analysis showed the predominance of carbonate-fluorapatite, along with secondary phases of carbonate-hydroxylapatite and hydroxylapatite.

Associated minerals such as calcite, dolomite, quartz, gypsum, and zeolite were also Identified, reflecting the influence of early diagenetic processes on the mineralogical composition of the deposits. Chemical analyses revealed high concentrations of (CaO) and P_2O), confirming the significant economic value of these phosphate deposits. Variations in the concentrations of MgO, Al_2O_3, and Fe_2O_3 among the sublayers were also observed, resulting from mineralogical and depositional heterogeneity. From an environmental perspective, the study demonstrated significant enrichment in trace elements, particularly cadmium (Cd), uranium (U), and chromium (Cr), with cadmium recording the highest enrichment factor (EF $\approx$ 49.600). Furthermore, the results of the geo-accumulation index (I-geo) represents an effective and relabel tool for assessing pollution levels and the accumulation for chemical elements in sediments and soil, moreover this index provides a precis quantitative assessment of the degree of metal contamination potential ecological risk index (PERI) confirmed that the studied deposits fall within the category of very high environmental risk, as the total risk index (RI)

exceeded 37.000. These findings highlight the necessity of considering environmental and aspects during the exploitation of these phosphate deposits. The enrichment of trace elements can be linked to the climatic and environmental changes associated with the Paleocene–Eocene Thermal Maximum (PETM), which created favorable depositional and geochemical conditions for the accumulation of these elements within the phosphorite deposits.

Reference

• Adriano, D. C. (2001). Trace elements in terrestrial environments: Biogeochemistry, bioavailability, and risks of metals. Springer.

• Altschuler, Z. S. (1980). The geochemistry of trace elements in marine phosphorites Part I. Characteristic abundances and enrichment. SEPM Special Publication. https://doi.org/10.2110/pec.80.29.0019

• Altschuler, Z. S., Clarke, R. S., & Young, E. J. (1958). Geochemistry of uranium in apatite and phosphorite. US Government Printing Office.

• Altschuler, Z. S., Berman, S., & Cuttitta, F. (1967). Rare earths in phosphorites—Geochemistry and potential recovery. Economic Geology, 62, 735-758.

• Alloway, B. J. (Ed.). (2012). Heavy metals in soils: Trace metals and metalloids in soils and their bioavailability (Vol. 22). Springer Science & Business Media.

• Arning, E. T., Birgel, D., Schulz-Vogt, H. N., et al. (2012). Lipid biomarker patterns of phosphogenic sediments from upwelling areas. Geobiology, 10, 331-348.

• Ashley, K., Cordell, D., & Mavinic, D. (2011). A brief history of phosphorus: From the philosopher's stone to nutrient recovery and reuse. Chemosphere, 84, 737-746. https://doi.org/10.1016/j.chemosphere.2011.03.001

• Bailey, J. V., Corsetti, F. A., Greene, S. E., et al. (2009). Sulfide-oxidizing bacteria and phosphogenesis in the Miocene Monterey Formation. Geology, 37, 419-422.

• Blanchard, R. (2000). Environmental geochemistry. Springer.

• Blès, J. L., & Fleury, J. J. (1971). Carte géologique 1/50 000 Morsott (178) et notice explicative. Publication Service Géologique de l'Algérie.

• Boulemia, S., Hadji, R., & Hamimed, M. (2021). Depositional environment of phosphorites in a semiarid climate region, case of El Kouif area (Algerian–Tunisian border). Carbonates and Evaporites, 36(3), 53.

• Boumaza, B., Kechiched, R., & Chekushina, T. V. (2021). Trace metal elements in phosphate rock wastes from the Djebel Onk mining area (Tébessa, eastern Algeria): A geochemical study and environmental implications. Applied Geochemistry, 127, 104910. https://doi.org/10.1016/j.apgeochem.2021.104910

• Boumaza, B., Kechiched, R., Chekushina, T. V., Benabdeslam, N., Senouci, K., Ait Merzeg, F., ... & Harizi, K. (2024). Geochemical distribution and environmental assessment of potentially toxic elements in farmland soils, sediments, and tailings from phosphate industrial area (NE Algeria). Journal of Hazardous Materials, 465, 133110. https://doi.org/10.1016/j.jhazmat.2023.133110

• Bradl, H. (Ed.). (2005). Heavy metals in the environment: Origin, interaction and remediation (Vol. 6). Elsevier.

• Brown Jr, G. E., & Parks, G. A. (2001). Sorption of trace elements on mineral surfaces: Modern perspectives from spectroscopic studies, and comments on sorption in the marine environment. International Geology Review, 43(11), 963-1073. https://doi.org/10.1080/00206810109465060

• Buccione, R., Kechiched, R., Mongelli, G., & Sinisi, R. (2021). REEs in the North Africa P-bearing deposits, paleoenvironments, and economic perspectives: A review. Minerals, 11(2), 214. https://doi.org/10.3390/min11020214

• Chaabani, F. (1995). Dynamique de la partie orientale du bassin de Gafsa au crétacé et au paléogène. Étude minéralogique et géochimique de la série phosphatée éocène (Tunisie méridionale). (Doctoral Thesis). Université Tunis.
• Chabou-Mostefai, S. (1987). Étude de la série phosphatée tertiaire du Djebel Onk, Algérie, Stratigraphie, Pétrographie, Minéralogie et Analyse Statistique. (Thèse Doctorat). Université de Droit, d'Économie et des Sciences d'Aix-Marseille, France.
• Cielensky, G., & Benchernine, A. (1987). Stratigraphy of the Djebel Onk phosphatic series. EREM Report.
• Cielensky, G., Benchernine, N., & Watkowski, T. (1988). Works of prospecting and assessment of phosphates in the region of Bir El Ater. Internal Report, EREM (Entreprise de Recherche et d'Exploration Minière), Algeria.
• Cook, P. J., & McElhinny, M. W. (1979). A reevaluation of the spatial and temporal distribution of sedimentary phosphate deposits in the light of plate tectonics. Economic Geology, 74(2), 315-330. https://doi.org/10.2113/gsecongeo.74.2.315
• Cook, P. J., & Shergold, J. H. (1984). Phosphorus, phosphorites and skeletal evolution at the Precambrian—Cambrian boundary. Nature, 308(5956), 231-236.
• Corbridge, D. (2016). Phosphorus: Chemistry, biochemistry and technology (6th ed.). CRC Press. https://doi.org/10.1201/b12961
• Dassamiour, M., Mezghache, H., Raji, O., & Bodinier, J. L. (2021). Depositional environment of the Kef Essennoun phosphorites (northeastern Algeria) as revealed by P2O5 modeling and sedimentary data. Arabian Journal of Geosciences, 14(12), 1078.
• Devallois, V. (2009). Transfert et mobilité des éléments traces métalliques dans la colonne sédimentaire des hydrosystèmes continentaux. (Doctoral dissertation). Aix-Marseille Université.
• Dong, S., et al. (2024). Phosphogenesis during Paleocene-Eocene thermal perturbations. Earth-Science Reviews.
• Dubourdieu, G. (1956). Étude géologique de la région de l'Ouenza. Publication Service Carte Géologique Algérie, ns(10), 41-285.
• Duffus, J. H. (2002). "Heavy metals"—A meaningless term? Pure and Applied Chemistry, 74(5), 793-807. https://doi.org/10.1351/pac200274050793
• Farr, T. D. (1950). Phosphate rock. U.S. Geological Survey Bulletin.
• Ferhaoui, S., Kechiched, R., Bruguier, O., Sinisi, R., Kocsis, L., Mongelli, G., ... & Laouar, R. (2022). Rare earth elements plus yttrium (REY) in phosphorites from the Tébessa region (Eastern Algeria): Abundance, geochemical distribution through grain size fractions, and economic significance. Journal of Geochemical Exploration, 241, 107058. https://doi.org/10.1016/j.gexplo.2022.107058
• Filippelli, G. M. (2008). The global phosphorus cycle: Past, present, and future. Elements, 4(2), 89-95. https://doi.org/10.2113/GSELEMENTS.4.2.89
• Filippelli, G. M. (2011). Phosphate rock formation and marine phosphorus geochemistry. Elements, 7, 89-95.
• Folk, R. L., & Ward, W. C. (1957). Brazos River bar: A study in the significance of grain size parameters. Journal of Sedimentary Petrology, 27, 3-26.

• Föllmi, K. B. (1996). The phosphorus cycle, phosphogenesis and marine phosphate-rich deposits. Earth-Science Reviews, 40(1-2), 55-124. https://doi.org/10.1016/0012-8252(95)00049-6
• Föllmi, K. B. (2016). Sedimentary phosphates revisited. Sedimentology, 63, 1-35.
• Galfati, I., Sassi, A. B., Zaier, A., Bouchardon, J. L., Bilal, E., Joron, J. L., & Sassi, S. (2010). Geochemistry and mineralogy of Paleocene-Eocene Oum el Khecheb phosphorites (Gafsa-Metlaoui basin) Tunisia. Geochemical Journal, 44(3), 189-210. https://doi.org/10.2343/geochemj.1.0062
• Garnit, H., Bouhlel, S., & Jarvis, I. (2017). Geochemistry and depositional environments of Paleocene–Eocene phosphorites: Metlaoui group, Tunisia. Journal of African Earth Sciences, 134, 704-736. https://doi.org/10.1016/j.jafrearsci.2017.07.021
• Glenn, C. R., Föllmi, K. B., Riggs, S. R., Baturin, G. N., Grimm, K. A., Trappe, J., & Siegmund, H. (1994). Phosphorus and phosphorites: Sedimentology and environments of formation. Eclogae Geologicae Helvetiae, 87(3), 747-788.
• Gunnars, A., Blomqvist, S., & Martinsson, C. (2004). Inorganic formation of apatite in brackish seawater from the Baltic Sea: An experimental approach. Marine Chemistry, 91(1-4), 15-26. https://doi.org/10.1016/j.marchem.2004.01.008
• Hakanson, L. (1980). An ecological risk index for aquatic pollution control: A sedimentological approach. Water Research, 14(8), 975-1001. https://doi.org/10.1016/0043-1354(80)90143-8
• Harouiya, N., & Oelkers, E. H. (2004). An experimental study of the effect of aqueous fluoride on quartz and alkali-feldspar dissolution rates. Chemical Geology, 205(1-2), 155-167. https://doi.org/10.1016/j.chemgeo.2004.01.005
• Harouiya, N., Chaïrat, C., Köhler, S. J., Gout, R., & Oelkers, E. H. (2007). The dissolution kinetics and apparent solubility of natural apatite in closed reactors at temperatures from 5 to 50 °C and pH from 1 to 6. Chemical Geology, 244(3-4), 554-568. https://doi.org/10.1016/j.chemgeo.2007.07.011
• Jarup, L. (2003). Hazards of heavy metal contamination. British Medical Bulletin, 68(1), 167-182. https://doi.org/10.1093/bmb/ldg032
• Jarvis, I., Burnett, W. C., Nathan, Y., Almbaydin, F. S. M., Attia, A. K. M., Castro, L. N., ... & Zanin, Y. N. (1994). Phosphorite geochemistry: State-of-the-art and environmental concerns. Eclogae Geologicae Helvetiae, 87(3), 643-700.
• Jasinski, S. M. (2024). Mineral commodity summaries: Phosphate rock. U.S. Geological Survey. https://doi.org/10.3133/mcs2024
• Kabata-Pendias, A. (2011). Trace elements in soils and plants (4th ed.). CRC Press.
• Kassatkine, Y., Yahyaoui, A., & Chatilov, S. (1980). The works of prospecting and assessment on phosphate executed in 1976–1978 in the mining district of Djebel Onk. SONAREM Internal Report, 2.
• Kechiched, R., Laouar, R., Bruguier, O., Kocsis, L., Salmi-Laouar, S., Bosch, D., & Larit, H. (2020). Comprehensive REE+Y and sensitive redox trace elements of Algerian phosphorites (Tébessa, eastern Algeria): A geochemical study and depositional environments tracking. Journal of Geochemical Exploration, 208, 106396. https://doi.org/10.1016/j.gexplo.2019.106396

• Kechiched, R., Laouar, R., Bruguier, O., Laouar-Salmi, S., Ameur-Zaimeche, O., & Foufou, A. (2016). Preliminary data of REE in Algerian phosphorites: A comparative study and paleo-redox insights. Procedia Engineering, 138, 19-29. https://doi.org/10.1016/j.proeng.2016.02.048
• Kechiched, R., Laouar, R., Bruguier, O., Salmi-Laouar, S., Kocsis, L., Bosch, D., ... & Larit, H. (2018). Glauconite-bearing sedimentary phosphorites from the Tébessa region (eastern Algeria): Evidence of REE enrichment and geochemical constraints on their origin. Journal of African Earth Sciences, 145, 190-200. https://doi.org/10.1016/j.jafrearsci.2018.05.018
• Kechiched, R., Sinisi, R., Kocsis, L., Bruguier, O., Mongelli, G., Ferhaoui, S., ... & Laouar, R. (2024). Phosphate deposits in North Africa: An overview of Algerian-Tunisian deposits, geochemistry and paleoenvironments. In The Geology of North Africa (pp. 471-499).
• Kocsis, L., et al. (2014). PETM-related phosphogenesis. Palaeogeography, Palaeoclimatology, Palaeoecology.
• Koschinsky, A., Stascheit, A., Bau, M., & Halbach, P. (1997). Effects of phosphatization on the geochemical and mineralogical composition of marine ferromanganese crusts. Geochimica et Cosmochimica Acta, 61(19), 4079-4094. https://doi.org/10.1016/S0016-7037(97)00231-7
• Krajewski, K. P. (2011). Sulfide bacteria and phosphorite formation. Sedimentary Geology.
• Lamboy, M., et al. (1994). Origin of phosphatic coprolites. Sedimentary Geology.
• Laouar, K., Laouar, R., Bruguier, O., Bosch, D., Kechiched, R., Bouhlel, S., & Tlili, A. (2024). Geochemistry of Bled El Hadba phosphorites (NE Algeria): Glauconitization process versus REE-enrichment. Journal of Geochemical Exploration, 258, 107398. https://doi.org/10.1016/j.gexplo.2024.107398
• Lucas, J., & Prévôt, L. (1981). Synthèse d'apatite à partir de matière organique phosphorée (ARN) et de calcite par voie bactérienne. Sedimentology, 28, 851-857.
• McKelvey, V. E. (1950). Geologic importance of phosphorites. Geological Society of America Bulletin.
• Morris, P. J., et al. (2011). Paleocene-Eocene Thermal Maximum and marine phosphorus cycle. Nature Geoscience.
• Nancollas, G. H. (1979). The growth of crystals in solution. Advances in Colloid and Interface Science, 10(1), 215-252. https://doi.org/10.1016/0001-8686(79)87007-4
• Nathan, Y. (1984). The mineralogy and geochemistry of phosphorites. In Phosphate minerals (pp. 275-291). Springer.
• Notholt, A. J. G., Sheldon, R. P., & Davidson, D. F. (Eds.). (1989). Phosphate deposits of the world, Vol. 2. Cambridge University Press.
• Omelon, S. J., & Grynpas, M. D. (2008). Relationships between polyphosphate chemistry, biochemistry and apatite biomineralization. Chemical Reviews, 108(11), 4694-4715. https://doi.org/10.1021/cr078252
• Ounis, A., Kocsis, L., Chaabani, F., & Pfeifer, H. R. (2008). Rare earth elements and stable isotope geochemistry (δ13C and δ18O) of phosphorite deposits in the Gafsa Basin, Tunisia. Palaeogeography, Palaeoclimatology, Palaeoecology, 268(1-2), 1-18. https://doi.org/10.1016/j.palaeo.2008.07.005
• Parian, M., & Cortiel, P. (1993). Étude de développement du gisement de phosphate de Djebel Onk (Algérie). Rapport d'expertise géologique, BRGM France, 288.
• Pirajno, F. (2008). Hydrothermal processes and mineral systems. Springer Science & Business Media.

• Piqué, A. (2002). The Mesozoic–Cenozoic Atlas belt (North Africa): An overview. Geodinamica Acta, 15(3), 185-208. https://doi.org/10.1016/s0985-3111(02)01088-4
• Pohl, W., & Groat, L. A. (2017). Mineral deposits of the world. Springer.
• Pufahl, P. K., Grimm, K. A., Abed, A. M., & Sadaqah, R. M. (2003). Upper Cretaceous (Campanian) phosphorites in Jordan: Implications for the formation of a south Tethyan phosphorite giant. Sedimentary Geology, 161(3-4), 175-205. https://doi.org/10.1016/S0037-0738(03)00070-8
• Pufahl, P. K., & Groat, L. A. (2017). Sedimentary and igneous phosphate deposits: Formation and exploration. Economic Geology, 112(3), 483-516. https://doi.org/10.2113/econgeo.112.3.483
• Rakovan, J., & Reeder, R. J. (1996). Intracrystalline rare earth element distributions in apatite: Surface structural influences on incorporation during growth. Geochimica et Cosmochimica Acta, 60(22), 4435-4445. https://doi.org/10.1016/S0016-7037(96)00244-X
• Ranchin, G. (1963). The sedimentary phosphates of lime in Djebel Onk's region (Algeria). SERM Paris, France, 85.
• Ruttenberg, K. C. (2003). The global phosphorus cycle. Treatise on Geochemistry, 8, 682. https://doi.org/10.1016/B0-08 043751-6/08153-6
• Ruttenberg, K. C. (2019). Phosphorus geochemistry in marine sediments. Annual Review of Marine Science.
• Saïd, A., Baby, P., Chardon, D., & Ouali, J. (2011). Structure, paleogeographic inheritance, and deformation history of the southern Atlas foreland fold and thrust belt of Tunisia. Tectonics, 30(6). https://doi.org/10.1029/2011TC002862
• Saouli, S., Kechiched, R., Bruguier, O., Mongelli, G., Bosch, D., Ameur-Zaimeche, O., & Laouar, R. (2025). Multi-scale (whole-rock, grain size, and particles) distribution of Potentially Hazardous Elements (PHEs) in sedimentary phosphorites from Algerian deposits: Geochemical and environmental implications. Journal of Hazardous Materials, 138414. https://doi.org/10.1016/j.jhazmat.2025.138414
• Sassi, S. (1974). La sédimentation phosphatée au Paléocène dans le Sud et le Centre Ouest de la Tunisie. (Thèse Doctorat). Université Paris Sud Orsay, France.
• Sassi, S. (1980). Phosphogenesis in the Tethyan realm. Sedimentary Geology.
• Shaban, A. (2016). A review on phosphate deposits. Natural Resources Research.
• Sheldon, R. P. (1963). Phosphorus in marine environments. U.S. Geological Survey Professional Paper.
• Sheldon, R. P. (1964). Paleogeography and phosphorite deposition. Geological Society of America Memoir.
• Simon, N. (2010). GRADISTAT user manual.
• Slansky, M. (1986). Geology of sedimentary phosphates. Elsevier.
• Sposito, G. (2008). The chemistry of soils (2nd ed.). Oxford University Press.
• Taylor, S. R., & McLennan, S. M. (1985). The continental crust: Its composition and evolution. Blackwell Scientific.
• Trappe, J. (Ed.). (1998). Phanerozoic phosphorite depositional systems: A dynamic model for a sedimentary resource system. Springer.
• Tyrrell, T. (1999). The relative influences of nitrogen and phosphorus on oceanic primary production. Nature, 400, 525-531. https://doi.org/10.1038/22941

• Van Kauwenbergh, S. J. (2010). World phosphate rock reserves and resources (p. 48). IFDC. https://hub.ifdc.org/handle/20.500.14297/1742
• Visse, L. (1952). Genesis of the southeasterly Algerian–Tunisian phosphatic deposits. XIX International Geological Congress, 1, 60.
• Zachos, J. C., Röhl, U., Schellenberg, S. A., Sluijs, A., Hodell, D. A., Kelly, D. C., ... & Kroon, D. (2005). The Paleocene-Eocene boundary in ODP Leg 208 sites. PANGAEA.
• Zaïer, A., Béji-Sassi, A., Sassi, S., & Moody, R. T. J. (1998). Basin evolution and deposition during the early Paleocene in Tunisia. In D. S. Macgregor, R. T. J. Moody, & D. D. Clark-Lowes (Eds.), Petroleum geology of North Africa (pp. 375-393). Geological Society, London, Special Publications.
• Zargouni, F. (1985). Tectonique de l'Atlas méridional de Tunisie, évolution géométrique et cinématique des structures en zone de cisaillement. (Thèse Doctorat ès-Sciences). Université Louis Pasteur.